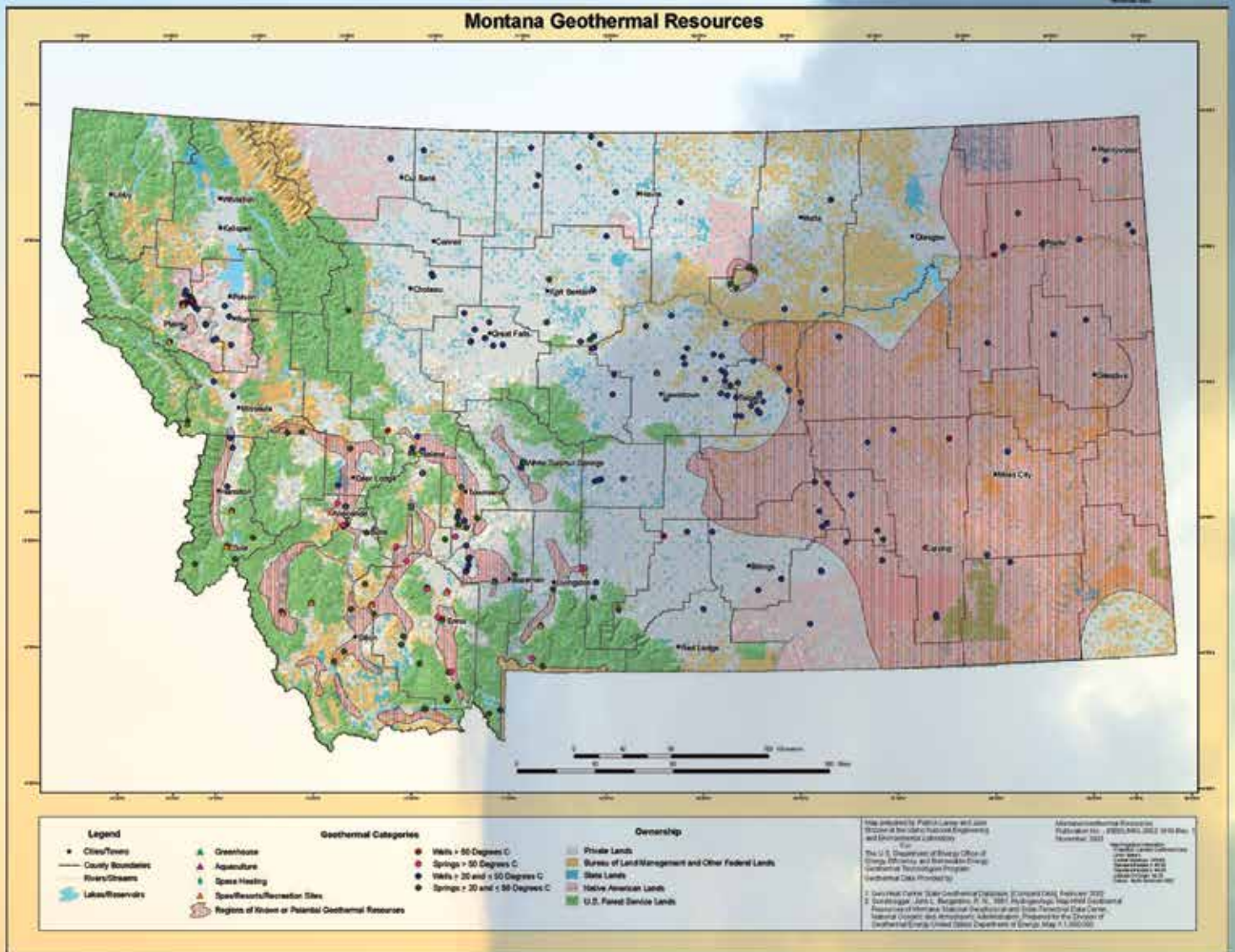




GEO-HEAT CENTER QUARTERLY BULLETIN



GEO THERMAL USE IN MONTANA

GEO-HEAT CENTER QUARTERLY BULLETIN

ISSN 0276-1084

*A Quarterly Progress and Development Report on the Direct Utilization of Geothermal Resources***CONTENTS**

- Comments from the Editor 1
Tonya “Toni” Boyd
- The Economic, Environmental, and Social 2
Benefits of Geothermal Use in Montana
Andrew Chiasson
- Technical Assessment of the Combined Heat 9
and Power Plant at the Oregon Institute
of Technology, Klamath Falls, Oregon
Tonya “Toni” Boyd and Ronald DiPippo
- Concentrated Solar and Geothermal Hybrid 16
Power Project
Guy Nelson and Garth Larsen
- Hybrid Geothermal and Solar Thermal 19
Power Plant Case Study; Gümüşköy GEPP
*Ö. Çağlan Kuyumcu, Umut Z.D. Solarğlu, Sertaç
Akar, Onur Serin*
- A Thermoelectric-Based Point of Use..... 25
Power Generator for Steam Pipes
*R. Dell, C.S. Wei, G. Sidebotham, Magnus Thor
Jonsson, and Rdnar Unnpórsson*
- Uses and Advantages of Geothermal 30
Resources in Mining
Piyush Bakane

PUBLISHED BY

GEO-HEAT CENTER
Oregon Institute of Technology
3201 Campus Drive
Klamath Falls, OR 97601
Phone: (541) 885-1750
E-mail: geoheat@oit.edu

EDITOR

Tonya “Toni” Boyd
Cover Design – SmithBates Printing & Design

WEBSITE:

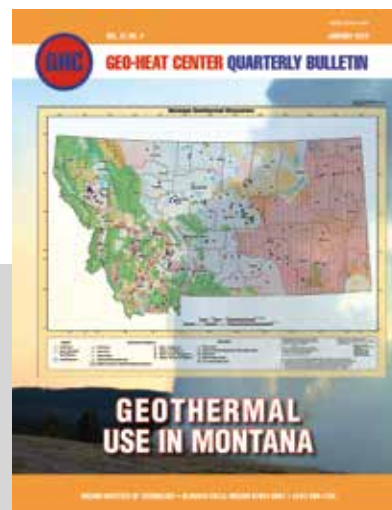
<http://geoheat.oit.edu>

ACKNOWLEDGEMENT

This material is based upon work supported by the Department of Energy (National Nuclear Security Administration) under Award Number DE-EE0002741.

DISCLAIMER

This *Bulletin* was prepared as an account of work sponsored by an agency of the United States government. Neither the United States Government nor any agency thereof, nor any of their employees, makes any warranty, express or implied or assumes any legal liability or responsibility for the accuracy, completeness, or usefulness of any information, apparatus, product or process disclosed, or represents that its use would not infringe privately owned rights. Reference herein any specific commercial product, process, or service by trade name, trademark, manufacturer, or otherwise does not necessarily constitute or imply endorsement recommendation, or favoring by the United States Government or any agency thereof.



Cover: *Geothermal Resources in Montana*

COMMENTS FROM THE EDITOR

Tonya "Toni" Boyd

GEO-HEAT CENTER QUARTERLY BULLETIN

We want to inform all our readers that this is the last issue of the Geo-Heat Center Quarterly Bulletin. January 2013 marks the end of our contract under Award Number DE-EE0002741. This contract allowed us to publish the Bulletin for three years (12 issues), prepare several state reports (Arizona, the Dakotas, Eastern States, Montana, Oregon, Washington and Wyoming) and to continue providing technical assistance to increase the utilization of geothermal energy in the U.S., especially in the areas of direct utilization.

BULLETIN HISTORY

The first issue of the Bulletin was published in May 1975. There have been three periods up to this point where funding was not available for the Bulletin. They occurred from Summer 1987 to the Summer 1988, from September 2005 to September 2006 and from January 2008 to May 2010. There have been three editors of the bulletin over the years: Paul Lienau, John Lund and myself.

The Geo-Heat Center has published almost 675 articles in 120 issues of the bulletin. The topics of the articles range from Aquaculture to Wells. Below are some of the subject headings:

Agribusiness, Aquaculture, Case Studies, Cooling, Economics, Education/Training, Electric Power, Equipment/Materials, Exploration/Evaluation, General Utilization, Geothermal Resources, Greenhouses, Heat Exchangers, Heat Pumps, Industrial, International, Metering, Miscellaneous, Resorts/Spas, Snow Melting; Space / District Heating and Wells.

The Geo-Heat Center started placing the bulletin articles online after they had been published since 1995. Since that time we have added older bulletin issues and articles. These all are available from our website at <http://geoheat.oit.edu/gcindex.htm>

NATIONAL GEOTHERMAL DATABASE SYSTEM

The Geo-Heat Center is working on another contract which is part of the National Geothermal Database System. Under this contract we are digitizing all the publications in our library, past bulletin articles, and technical papers. We will be including metadata information for the publications and placing them online to be accessible through our library website and also the National Geothermal Database System website.

The webpage location for the Geo-Heat Center library publications is <http://digitalib.oit.edu/cdm/landingpage/collection/geoheat>

GHC BULLETIN, JANUARY 2013

The webpage location for the National Geothermal Database System is <http://www.geothermaldatabase.org>. This website will include all the data and publications from all the contributors for the National Geothermal Database System.

The Geo-Heat Center has been able to hire several students from the Oregon Institute of Technology to help with the completion of this contract by scanning and inputting the metadata information. The picture below was taken at the Geothermal Resource Council Annual Meeting in Oct. 2012 which most of the students were able to attend.



Geo-Heat Center students, staff and emeritus at the Geothermal Resources Council Annual Meeting 2012. From left to right: Reginald Boyle, Phillip Maddi, Todd Krueger, Seth Lutz, Sam Cole, Greg Robinson, Sarah Hole, Ziyad El Tawil, Spencer Jones, Jon Hall, Aleena Anderson, Nick DeMolina, Toni Boyd (staff), Andrew Zvibleman and John Lund (emeritus). Not pictured: Andrew Chiasson, Joe Miranda, Casey Coulson, and Matt Perkins.

GEOTHERMAL ENERGY PROSPECTING FOR THE CARIBBEAN ISLANDS OF NEVIS AND MONTserrat

It was brought to our attention that the bulletin article referenced above published in the *GHC Quarterly Bulletin* Vol. 31, No. 2 was not properly referenced concerning some of the figures and text. Below is the acknowledgment by the author and apology.

E-mail from Randy R. Koon Koon

I am emailing you with regards to the article "Geothermal Energy Prospecting for the Caribbean Islands of Nevis and Montserrat" in the *Geo-Heat Center Quarterly Bulletin* entitled "National Geothermal Academy" (ISSN 0276-1084, VOL. 31 NO. 2, AUGUST 2012). The figures and text in the paper I submitted are the original work of Dr. Joe LaFleur and Dr. Roland Hoag entitled "Geothermal Exploration on Nevis: A Caribbean Success Story" published in the Geothermal Resources Council (GRC) Transactions, Volume 34 in 2010. Hence the reader should reference the original GRC publication, rather than the paper in the above mentioned *GHC Quarterly Bulletin*.

THE ECONOMIC, ENVIRONMENTAL, AND SOCIAL BENEFITS OF GEOTHERMAL USE IN MONTANA

Andrew Chiasson, Geo-Heat Center, Oregon Institute of Technology, Klamath Falls, Oregon

Montana has a long and rich history of utilization of its geothermal resources. Today, the documented direct uses of geothermal waters are related to tourism and recreation, spas and resorts, space heating, and greenhouse heating. The Montana Department of Environmental Quality has recently published a consumer's guide to geothermal energy in Montana (Birkby, 2012), outlining the current and potential uses and advantages of geothermal energy in the State.

Geothermal resources for direct-utilization in Montana generally occur in the western and the eastern thirds of the state. In the western third of the state, geothermal features are related to Yellowstone National Park and the Rocky Mountains, where numerous hot springs are found. In the eastern third of the state, geothermal occurrence is different, and is related to the Williston Basin – a deep sedimentary basin extending through western North and South Dakota, eastern Montana, and southern Saskatchewan known for its rich deposits of petroleum.

ECONOMIC BENEFITS

The greatest use of geothermal energy today in Montana is related to spas and resorts, and recreation and tourism. Much of the other significant direct uses of geothermal energy (eg. space heating and greenhouse heating) stem from uses at spas and resorts.

A large contributor to the economic benefit of geothermal energy in Montana is also related to its historic entrance to Yellowstone National Park - a place that has made famous the marvels of geothermal energy. The town of Gardiner in southwest Montana boasts the only year-round entrance to the Park through The Roosevelt Arch (Figure 1), which was dedicated by President Theodore Roosevelt on 24 April 1903.

According to U.S. National Park Statistics, Yellowstone National Park currently attracts about 3 million recreational visitors per year, providing an enormous contribution to the region's economy. Since Yellowstone was designated a National Park in 1872 (America's first national park), over 156 million people have visited the park as of the end of 2011.

Numerous hot springs exist to the north and northwest of Yellowstone National Park, in the western third of Montana. Birkby (1999) lists 26 hot springs in western Montana in addition to four in the eastern part of the state. Of these, many are remote and not fully developed; this report summarizes only those that currently support viable businesses.

For many centuries, Native Americans gathered at natural hot springs to absorb the healing benefits that they believed came from soaking in the warm mineral water. Hot springs

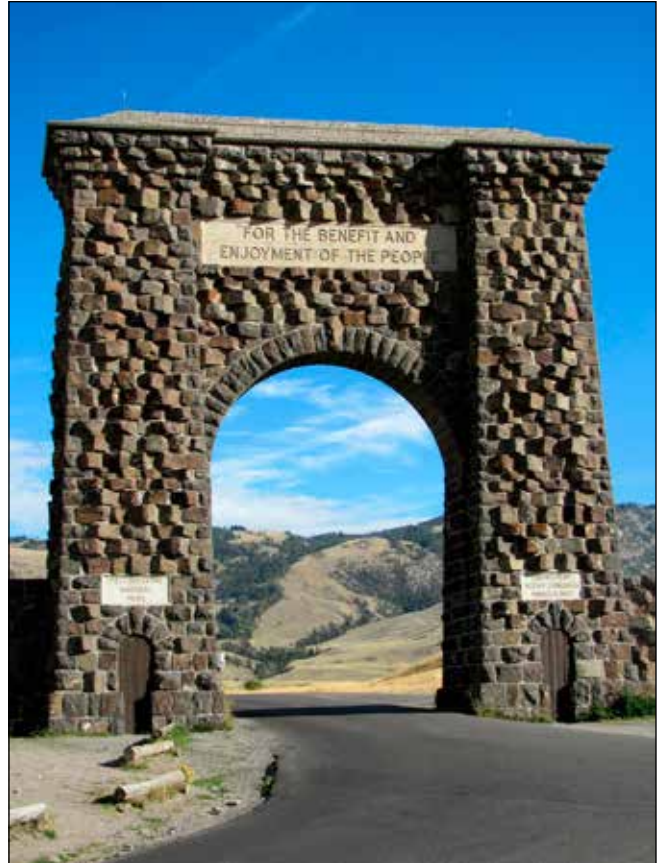


Figure 1. Historic Roosevelt Arch in Gardiner, Montana at the north entrance to Yellowstone National Park (www.gardiner-montana.com).

areas were regarded as sacred, neutral territory, and members of different tribes who encountered each other at a hot spring would put down their weapons and relax in peace. According to Jeff Birkby quoted in Martin (2012), “when John Bozeman, one of Montana’s first settlers, drove his wagon train by what would later become Hunter’s Hot Springs in 1864, one of the men with him reported seeing more than a thousand teepees of the Crow Indians camped there.”

Lewis and Clark are believed to be the first white settlers to encounter Montana’s hot springs when they camped near Lolo Hot Springs in 1805. Other explorers, trappers, and miners who passed through the state used the springs to bathe and wash clothes, and as Montana experienced a boom during the gold rush of the 1860s through the 1880s, crude bathhouses and log cabins were built near hot springs. Entrepreneurs eventually took advantage of the hot springs, particularly when the western railroad was built through Montana, and transformed the crude bathhouses into luxury resorts. These resorts often advertised miraculous medical cures to lure guests, and claimed to treat ailments of all kinds, from arthritis to liver disease.

As Montana developed and prospered, the state experienced an age of extravagant bathhouses from about 1890 to 1920. One of the most lavish was the Broadwater Hotel and Natatorium near Helena (Figure 2). According to Birkby (1999) “the palatial resort fulfilled Charles Broadwater’s ideals of elegance and refinement with Persian rugs covering the floors and French wallpaper lining the walls. After meals of up to ten courses served in the elegant dining room, guests could repose in parlors filled with Victorian furniture.”

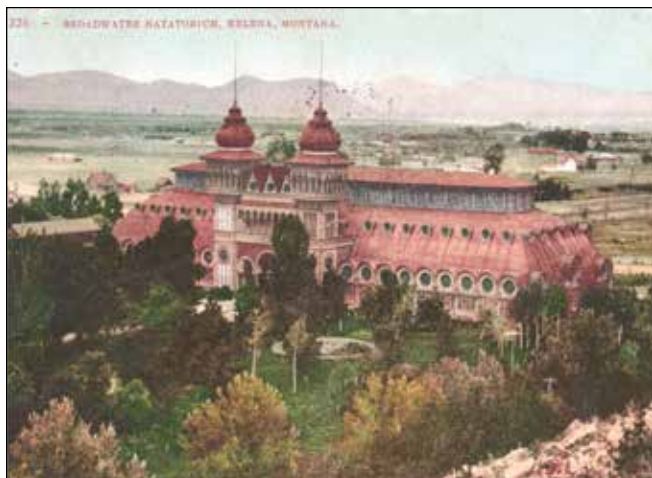


Figure 2. Broadwater Natatorium near Helena, circa 1889. (source: Birkby, 2012).

The elegant resorts of Montana entered a period of decline beginning in the 1920s due to a number of factors: population growth in the state failed to meet expectations, prohibition was enacted, and several of the resorts were irreparably damaged by fires and the historic earthquake that rocked the Helena area in 1935 (Martin, 2012).

Today, Boulder Hot Springs and Chico Hot Springs Resort, built in 1891 and 1900, respectively, are the only lavish resorts that remain from this period. There are also a number of smaller, family-owned resorts that exist, as well as springs on public land that are available for public use.

Boulder Hot Springs, having undergone major renovations since its original construction, today boasts an inn, indoor and outdoor pools, spa, and conference facilities. Chico Hot Springs, located just north of Yellowstone National Park, today offers lodges, log cabins, chalets, cottages, geothermal spring-fed pools, a mineral spa, and numerous amenities.

Bozeman Hot Springs, a small pool enjoyed only by a few in the late 1800’s, has evolved into a destination spot. Located minutes from Yellowstone National Park and Big Sky Resort, the facility features nine different pools (Figure 3) with temperatures ranging from 59 to 106°F, and both dry and wet saunas. To ensure a consistently clean facility, the indoor pools use a flow-through system so no chemicals are needed; they are drained and cleaned every night.

Fairmont Hot Springs, located off Interstate 90 between Yellowstone and Glacier National Parks claims a reputation throughout the Northwest for its pools. The facility boasts



Figure 3. Outdoor pool at Bozeman Hot Springs. (source: <http://www.bozemanhotsprings.co>)

two oversized Olympic swimming pools and two mineral soaking pools, one of each located indoors and outdoors. The pools are fed by 155°F natural hot spring water. The facility also offers a lodge, convention and events center, fitness center, and numerous amenities.

Jackson Hot Springs in the heart of the Big Hole Valley offers an approximate 10,000 sq. ft. rustic lodge and outdoor warm-water pool (approximately 30 ft x 75 ft) fed by the 137°F hot springs. The geothermal spring, located about 1,300 feet east of the lodge, is almost odorless, with no trace of sulfur smell. As such, the water is piped underground to the town of Jackson, and serves as the town’s source of water. According to Birkby (1999), Jackson Hot Springs hosted celebrities, including Bing Crosby and Bob Hope, and the Lewis and Clark expedition passed by this area on their return from the Pacific Ocean.

Lolo Hot Springs is located southwest of Missoula in the Bitterroot region of Montana next to the Idaho border. The hot springs were well known to Native Americans, as a mineral lick for wild game and an ancient meeting place. Lewis and Clark visited there in 1805 and again on their return trip in 1806. The hot, mineralized springs became a landmark and rendezvous point for early explorers, and by 1885, Lolo Hot Springs had become a favorite vacationing spot for new homesteaders. Today, there is a large outdoor swimming pool, and indoor soaking pool, both heated by geothermal springs. There is also a hotel, restaurant, saloon, RV park, camping and picnicking area, and an extensive trail system. The Lolo Hot Springs produce 275,000 gallons of water per day at temperatures between 104 and 117°F. The hot water is collected in a 35,000 gallon holding tank which is used to supply drinking and shower water for the restaurant, hotel, swimming pool, and other establishments in the area (Lund, 2002). Water from the springs is used directly for filling the pool and for heating the decks and floors of the pool area (Lund, 2002).

The Lost Trail Hot Springs Resort is a rustic hot springs resort in a narrow, pine-covered mountain valley along the Lewis and Clark Trail. The 110°F hot springs are located on a hillside approximately 0.75 mile above the resort and are piped directly into a 25 ft x 75 ft outdoor swimming pool and an adjoining indoor hot tub. Unlike many hot springs in Montana, the water at Lost Trail is odorless, with no sulfur

smell. Pool temperatures average 95°F year-round, and the temperature averages 105°F in the hot tub. The resort also offers a restaurant and many outdoor recreation activities.

Norris (also known as Bear Trap) Hot Springs is a natural hot pool that has been in use since ancient Indians wintered in the area. The springs later served as a day trip destination for train travelers in the early 1900's when there was a booming local gold mine. Today, the 30 ft x 40 ft open-air wooden pool has changed little since the 1880s. Eight to ten separate springs with an average temperature of 127°F feed the pool at a flow-through rate of about 500,000 gallons of water per day. The odor-free hot water is air-cooled by forcing it through a small vertical pipe at one end of the pool; natural artesian pressure shoots the water out of the pipe in a graceful 12-foot arc above the pool, creating a constant hot water shower on the bathers below (Birkby 1999).

Quinn's Hot Springs Resort has six pools for soaking and swimming. Four soaking pools range in temperature from 60 to 106°F. Swimming pools (Figure 4) typically range in temperature from 80 to 95°F. All pools are monitored for cleanliness and temperature every three hours and adjusted as necessary. The resort offers several amenities, including dining and an events center.



Figure 4. Outdoor mineral/swimming pool at Quinn's Hot Springs (source: [www. http://quinnshotsprings.com/ Pools.aspx](http://quinnshotsprings.com/Pools.aspx))

Sleeping Buffalo Hot Springs in northeast Montana was discovered in 1922, when oil exploration drilling encountered a tremendous flow of hot mineral water at 3,200 feet. Legend has it that cowboys used the hot water for their Saturday night baths. The hot springs were named in honor of a particular rock resembling a buffalo which signifies the staff of life for several Native American tribes. Sleeping Buffalo resort includes two indoor pools: an 8 ft x 26 ft hot pool kept at about 106°F, and a 50 ft x 60 ft swimming pool kept at about 90°F. The indoor pools are open year-round. The geothermal water comes from a well about 3,200 feet deep that flows 750 gallons per minute of 106°F water. The resort also offers hotel rooms, cabins, a café, gift shop, and banquet rooms.

Spa Hot Springs Motel and Clinic, located in the city limits of White Sulphur Springs in southwest Montana, is owned by Dr. Gene Gudmundson, D.C., a licensed chiropractor. Thermal water for the pools and motel is of high sulfur content, and is provided by a 130°F geothermal well drilled near the site of the original springs. The outdoor pool is kept at 98°F in the

winter and 96°F in the summer. A 105°F indoor soaking pool is located near the main pool. The Spa Motel has 21 guest rooms, a natural health clinic, and several nearby attractions.

Symes Hot Springs and Mineral Baths are located near the town of Hot Springs in northwest Montana. The facility has three available pools kept at a hot (107°F), medium (101°F), and warm temperature (95°F) that are fed by geothermal springs at about 120°F. The Symes Hotel is a registered landmark; it features a restaurant, massage treatments, and many other amenities.

In addition to the numerous recreational and therapeutic uses of geothermal waters in Montana, there are many documented and undocumented uses of geothermal energy for space heating. Many of the documented uses are related to spas and resorts, with almost all of the larger resorts using their geothermal water to provide space heating for their hotels and their laundry needs. In addition, the laundry water at Warm Spring State Hospital northwest of Butte is preheated with geothermal water, saving a considerable amount of state tax dollars that would otherwise be spent on fossil fuel (Birkby, 2012). The Ennis RV Park near Ennis uses the hottest spring found in Montana at 180°F to provide hot water to vacationers for showers and laundry.

Major resorts in Montana using geothermal energy to heat their buildings include Boulder Hot Springs Inn and Spa (Figure 5), Bozeman Hot Springs, Chico Hot Springs Resort and Day Spa (Figure 6), Fairmont Hot Springs Resort, the Symes Hotel, and the Spa Hot Springs Motel and Clinic in White Sulphur Springs. Individual homes near hot springs also are heated with geothermal energy, including homes in Helena and the Bitterroot Valley north of Hamilton (Birkby, 2012). At Sleeping Child Hot Springs in the Bitterroot National Forest near Hamilton, a 25,000 sq. ft. exclusive living space is heated with geothermal springs on the property.



Figure 5. The Inn at Boulder Hot Springs. (source: <http://www.boulderhotsprings.com>).

Greenhouse heating, another popular use of geothermal resources, is used at a few Montana locations. Chico Hot Springs Resort has had a geothermally-heated greenhouse (Figure 7) in operation for several years. The fresh herbs,

flowers, and vegetables grown in this greenhouse are featured in many of the menu items in Chico's gourmet restaurant (Birkby, 2012).

Greenhouse heating, another popular use of geothermal resources, is used at a few Montana locations. Chico Hot Springs Resort has had a geothermally-heated greenhouse (Figure 7) in operation for several years. The fresh herbs, flowers, and vegetables grown in this greenhouse are featured in many of the menu items in Chico's gourmet restaurant (Birkby, 2012).



Figure 6. Chico Hot Springs Resort. (source: Birkby, 2012).



Figure 7. A year-round banana tree grown in a geothermal greenhouse at Chico Hot Springs Resort. (source: Birkby, 2012)

At Silver Star Hot Springs in southwestern Montana, a 30 ft x 120 ft geothermal greenhouse has been raising organic tomatoes since the early 2000s (Figure 8). The greenhouse owners have found a niche market selling their product to local farmers' markets and restaurants in Bozeman and Butte (Birkby, 2012).

Madison Farm-to-Fork, an initiative to encourage and promote local food growing in Madison County, has completed two approximately 70 ft x 40 ft greenhouses in 2011 near Ennis (Figure 9). The greenhouses are heated using geothermal fluids at about 180°F issuing from Ennis Hot Springs. The current plan calls for one greenhouse to be used for food production, and the other as a facility to teach school children the skills and benefits of growing their own food.



Figure 8. Organic tomatoes grown in a geothermal greenhouse at Silver Star Hot Springs. (source: http://grannysstore.com/Silver_Star_About.htm)



Figure 9. Madison Farm-to-Fork greenhouse at Ennis Hot Springs. (source: www.madisonfarmtofork.com/mf2f-geothermal-greenhouse.html)

The numerous geothermal-related activities in Montana employ many people directly and indirectly. Geothermal uses significantly contribute to Montana's tourism economy, bringing revenue to the state, and creating many direct and indirect jobs. The use of geothermal energy that directly employs the most people in Montana is clearly related to the resort, spa, and recreation industry. Were it not for the many hot springs in Montana, these resorts would probably not exist. Using a standard multiplier of 2.5, geothermal businesses create an estimated 325 direct, indirect, and induced jobs in Montana.

Geothermal systems used for space heating are generally low-maintenance, and therefore employ only a few folks that are qualified to work on them. However, space heating of buildings and other applications using geothermal energy for heat results in significant energy cost savings to building and

business owners, which, in turn, results in money that can be kept in the local economy. Based on average 2012 natural gas prices, geothermal energy saves about \$1 million in annual energy costs for documented geothermal space-heating applications, and about \$1.8 million annually in the heating of spa and swimming pool water.

ENVIRONMENTAL BENEFITS

In addition to energy savings, geothermal energy usage prevents the emissions of greenhouse gases (GHG) and air pollutants, helping to keep a healthy living environment. If these activities used fossil fuels to generate the heat that geothermal water provides, they would emit at least 56,900 tonnes of carbon dioxide equivalent each year (Table 1) — the equivalent of removing 11,100 passenger vehicles from the road, saving 132,300 barrels of oil, and saving 12,100 acres of pine forest.

SOCIAL BENEFITS

Social benefits of direct-use geothermal utilization are difficult to measure quantitatively, but Jeff Birkby may be one of the first to undertake a social scientific assessment of the role of hot springs in the social fabric of societal development of Montana. The hot springs of Montana, Birkby says in Martin (2012), “often were the early social gathering areas of the state, where people would come for a bath on a weekend. The miners would gather there and tell stories . . . and so they became the early social centers.”

Today, hot springs resorts still serve as social centers. Another key social benefit from geothermal energy use in Montana is improved quality of life through recreation and spa therapy. Geothermal sources provide many unique recreational opportunities enjoyed by tens of thousands of people each year, attracting tourists to the state. Given the history of the geothermal spa industry, social benefits have been evident for many past generations. Providing a grand entrance to Yellowstone National Park, this area has provided unique educational opportunities of geothermal features to people worldwide.

THE FUTURE

Montana has significant geothermal potential for future uses, from new applications of direct use heating, to resurgence in mineral spa therapy, to development of low-to-moderate temperature resources for electrical power generation.

The Geo-Heat Center lists 18 communities in Montana that are within five miles of a geothermal resource with a temperature of 122°F or greater, making them possible candidates for district heating or other geothermal use. Also, Montana has a rich history related to the balneological use of geothermal waters, a practice which appears to be making a comeback. The southwestern, western, and eastern portions of the State have semi-developed springs and/or previously-developed springs from Montana’s grand era of bathhouses around the turn of the 20th century that are not currently commercially operational. Some of these areas

could be readily turned into viable businesses when the right buyers and market emerge. For example, Hunters Hot Springs near Livingston, once the site of the elegant Hotel Dakota in the early 1900s and a now-vanished bottled water plant, contains many thermal springs that produce one of the largest flows of hot water in Montana at more than 1,300 gallons per minute of 139°F water.

The potential of electricity generation from co-produced geothermal fluids from Montana’s oil fields is significant. Research and interest continues in the concept of generating electricity from co-produced fluids from deep petroleum wells in the Williston Basin, a portion of which underlies eastern Montana.

ACKNOWLEDGEMENTS

This material is based upon work supported by the Department of Energy under Award Number DE-EE0002741.

DISCLAIMER

This report was prepared as an account of work sponsored by an agency of the United States Government. Neither the United States Government nor any agency thereof, nor any of their employees, makes any warranty, express or implied, or assumes any legal liability or responsibility for the accuracy, completeness, or usefulness of any information, apparatus, product, or process disclosed, or represents that its use would not infringe privately owned rights. Reference herein to any specific commercial product, process, or service by trade name, trademark, manufacturer, or otherwise does not necessarily constitute or imply its endorsement, recommendation, or favoring by the United States Government or any agency thereof. The views and opinions of authors expressed herein do not necessarily state or reflect those of the United States Government or any agency thereof.

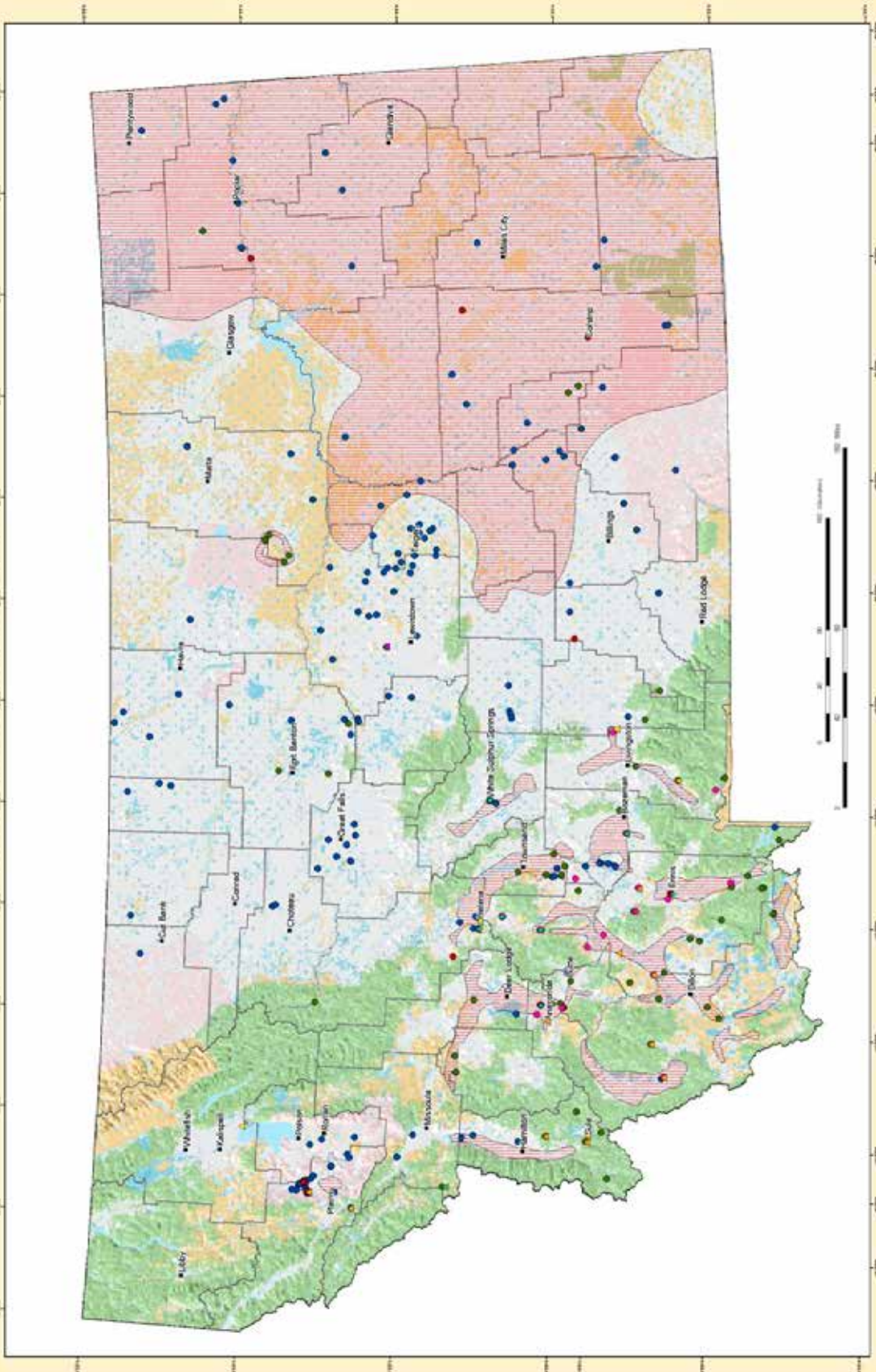
REFERENCES

- Birkby, J., 1999. *Touring Montana and Wyoming Hot Springs*. Falcon Publishing, Inc., Helena, Montana.
- Birkby, J., 2012. *Geothermal Energy in Montana - A Consumer’s Guide*. Montana Department of Environmental Quality, Energy & Pollution Prevention Bureau, Energy Planning & Renewables Section, Helena, Montana.
- Lund, J.W., 2002. Lolo Hot Springs, Montana. *Geo-Heat Center Quarterly Bulletin*, Vol. 23, No. 2.
- Lund, J.W., Freeston, D.H., and Boyd, T.L., 2010. *Direct Utilization of Geothermal Energy 2010*.
- Martin, E., 2012. Big Sky Oasis. *Humanities Magazine*, Vol. 33, No. 1.

Table 1. Energy Production and Carbon Emissions Offsets by Geothermal Energy Utilization in Montana.

| Site | Location | Application | Temp. (F) | Annual Energy Use | | Annual Emission Offsets (metric tonnes) | | |
|-------------------------------|-----------------------|-------------|-----------|--------------------------|-----------------------|---|-----------------|-----------------|
| | | | | (10 ⁹ Btu/yr) | (10 ⁶ kWh) | NO _x | SO _x | CO ₂ |
| Silver Star Hot Springs | Silver Star | Greenhouse | NA | 0.3 | 0.1 | 0.1 | 0.1 | 81 |
| Ennis Hot Springs | Ennis | Greenhouse | 180° | 0.5 | 0.1 | 0.2 | 0.2 | 136 |
| Chico Hot Springs | Pray | Greenhouse | 110° | 0.3 | 0.1 | 0.1 | 0.1 | 81 |
| Norris (Bear Trap) Hot Spring | Norris | Resort/Pool | 130° | 24 | 7.1 | 11 | 11.7 | 6,593 |
| Boulder Hot Springs | Boulder | Resort/Pool | 151° | 7.0 | 2.1 | 3.2 | 3.4 | 1,899 |
| Bozeman Hot Springs | Bozeman | Resort/Pool | 142° | 7.0 | 2.1 | 3.2 | 3.4 | 1,899 |
| Broadwater Hot Spring | Helena | Resort/Pool | 153° | 7.0 | 2.1 | 3.2 | 3.4 | 1,899 |
| Camas Hot Springs | Hot Springs | Resort/Pool | 104° | 0.7 | 0.2 | 0.3 | 0.3 | 190 |
| Wild Horse Hot Springs | Hot Springs | Resort/Pool | 124° | 7.0 | 2.1 | 3.2 | 3.4 | 1,899 |
| Chico Hot Springs | Park County | Resort/Pool | 113° | 4.6 | 1.3 | 2.1 | 2.2 | 1,248 |
| Elkhorn Hot Springs | Polaris | Resort/Pool | 140° | 7 | 2.1 | 3.2 | 3.4 | 1,899 |
| Fairmont Hot Springs Resort | Anaconda | Resort/Pool | 143° | 28 | 8.2 | 12.7 | 13.4 | 7,570 |
| Jackson Hot Springs | Jackson | Resort/Pool | 137° | 7.0 | 2.1 | 3.2 | 3.4 | 1,899 |
| Lolo Hot Springs Resort | Lolo | Resort/Pool | 117° | 7.0 | 2.1 | 3.2 | 3.4 | 1,899 |
| Lost Trail Hot Springs Resort | Sula | Resort/Pool | NA | 7.0 | 2.1 | 3.2 | 3.4 | 1,899 |
| Quinn's Hot Springs | Paradise | Resort/Pool | 120° | 7.0 | 2.1 | 3.2 | 3.4 | 1,899 |
| Sleeping Buffalo Hot Springs | Saco (10 mi. E) | Resort/Pool | 106° | 7.0 | 2.1 | 3.2 | 3.4 | 1,899 |
| Sleeping Child Hot Springs | Ravalli County | Resort/Pool | 125° | 2.5 | 0.7 | 1.1 | 1.2 | 678 |
| Spa Motel | White Sulphur Springs | Resort/Pool | 120° | 7.0 | 2.1 | 3.2 | 3.4 | 1,899 |
| Symes Hotel and Springs | Hot Springs | Resort/Pool | 90° | 7.0 | 2.1 | 3.2 | 3.4 | 1,899 |
| Ennis RV Park | Ennis | Space Htg. | 180° | 1.7 | 0.5 | 0.8 | 0.8 | 461 |
| Warm Springs State Hospital | Warm Springs | Space Htg. | 154° | 15 | 4.3 | 6.6 | 7.0 | 3,961 |
| Sleeping Child Hot Springs | Ravalli County | Space Htg. | 125° | 1.3 | 0.4 | 0.6 | 0.6 | 339 |
| Bozeman Hot Springs | Bozeman | Space Htg. | 131° | 5.8 | 1.7 | 2.6 | 2.8 | 1,574 |
| Broadwater Athletic Club | Helena | Space Htg. | 153° | 5.6 | 1.6 | 2.5 | 2.7 | 1,519 |
| Fairmont Hot Springs Resort | Anaconda | Space Htg. | 160° | 14 | 4.2 | 6.6 | 7.0 | 3,934 |
| Jackson Hot Springs Lodge | Jackson | Space Htg. | 137° | 2.9 | 0.8 | 1.3 | 1.4 | 787 |
| Lolo Hot Springs | Missoula Cnty. | Space Htg. | 111° | 13 | 3.7 | 5.7 | 6.1 | 3,419 |
| Spa Motel and Clinic | White Sulfur Springs | Space Htg. | 136° | 1.3 | 0.4 | 0.6 | 0.6 | 353 |
| Boulder Hot Springs | Boulder | Space Htg. | 169° | 4.4 | 1.3 | 2.0 | 2.1 | 1,194 |
| TOTALS | | | | 210 | 61 | 95 | 101 | 56,911 |

Montana Geothermal Resources



Legend

- City/Towns
- County Boundaries
- Rivers/Streams
- Lake/Reservoirs

Geothermal Categories

- Geysers
- Agriculture
- Spas/Healing
- Spas/Resorts/Recreation Sites
- Regions of Known or Potential Geothermal Resources

Temperature Zones

- Wells > 50 Degrees C
- Wells > 20 and < 50 Degrees C
- Wells > 150 and < 200 Degrees C
- Wells > 200 and < 300 Degrees C

Ownership

- Private Lands
- Bureau of Land Management and Other Federal Lands
- State Lands
- Native American Lands
- U.S. Forest Service Lands

Metadata:
 Map prepared by: David Lamm and Julie
 RTI Environmental Laboratory
 For:
 The U.S. Department of Energy, Office of
 Energy Efficiency and Renewable Energy
 Geothermal Technologies Program
 Geothermal Data Repository
 1. Geothermal Resource Assessment Database, February 2012, 4 February 2012
 2. Geothermal Resource Assessment Database, February 2012, 4 February 2012
 National Geospatial-Intelligence Agency, 2013
 National Geospatial-Intelligence Agency, 2013
 Geothermal Energy United States Department of Energy, Map 1 (2013)

TECHNICAL ASSESSMENT OF THE COMBINED HEAT AND POWER PLANT AT THE OREGON INSTITUTE OF TECHNOLOGY, KLAMATH FALLS, OREGON

Tonya “Toni” Boyd, Geo-Heat Center, Oregon Institute of Technology, Klamath Falls, Oregon
Ronald DiPippo, Renewable Energy Consultant, South Dartmouth, Massachusetts

ABSTRACT

The recently installed combined heat-power (CHP) plant at the Oregon Institute of Technology is described and its performance analyzed using thermodynamic First and Second Law principles based on energy and exergy, respectively. Characteristics of the three production and two injection wells are presented. Real-time plant data for the binary cycle and heating system are shown in a screen-shot from the control panel and used to carry out a system analysis. Both the power cycle by itself and the whole CHP system are assessed. The R245fa working-fluid power cycle is shown to have a thermal efficiency of 8.2% and a utilization efficiency of 33.5% relative to the exergy change of the geofluid, and the CHP system has an efficiency of 83.6%, using geofluid pumped to the plant at 196.9°F.

BRIEF HISTORY OF GEOTHERMAL ENERGY USAGE AT OIT

For over one hundred years, the people of Oregon have been using geothermal energy to heat buildings, melt snow from sidewalks, grow plants in greenhouses, and more. Situated 25 miles north of the border with California (see Figure 1), the community of Klamath Falls lies atop a particularly abundant supply of geothermal energy. One thousand homes are heated with hot water obtained from nearly 600 wells.

The existence of these geothermal resources was the motivation behind Oregon Institute of Technology (OIT) moving its Klamath Falls campus in 1964 to its present location in the northern part of the city. Specifically, the newly-constructed school was designed to tap hot water from the geothermal reservoir to heat campus buildings. Today that geothermal district heating system serves sixteen buildings totaling roughly 818,200 square feet of floor space at OIT (see Figures 2 and 3).

The institute is the only 100% geothermally-heated campus in North America. Now, with the inauguration of its first combined heat and power plant (CHP), OIT is well on its way to becoming not only geothermally heated but also geothermally electric powered with geothermal resources found on its own property. When this effort is brought to completion, this will set OIT apart from all other institutions of higher education in the world.

PRODUCTION AND INJECTION WELLS

There are three production wells in service to supply the OIT CHP plant: OIT-2, -5 and -6. Two injection wells receive the waste geofluid from the heating system: OITINJ-1 and -2. These are shown in the campus layout map in Figure 3. Selected information of these wells is given in Table 1.

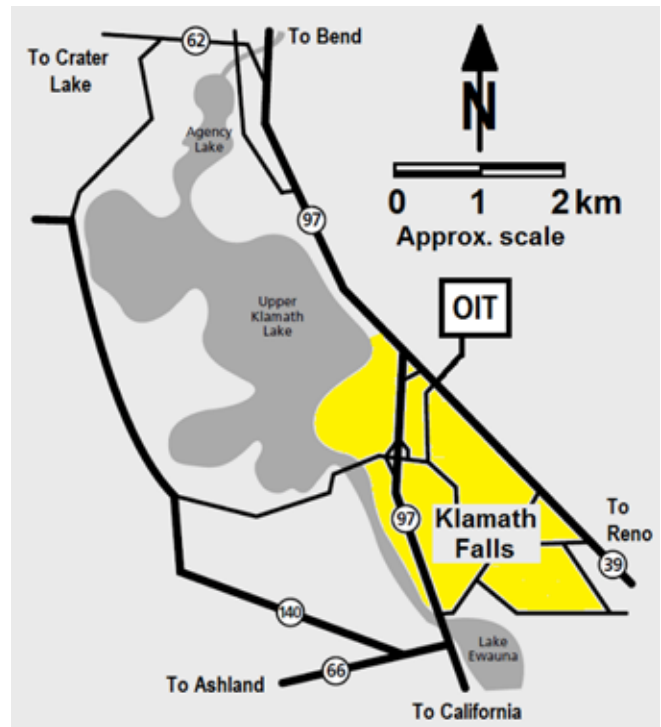


Figure 1. Location map for OIT.



Figure 2. Aerial view of OIT campus and CHP plant [Google Earth image, August 8, 2011].

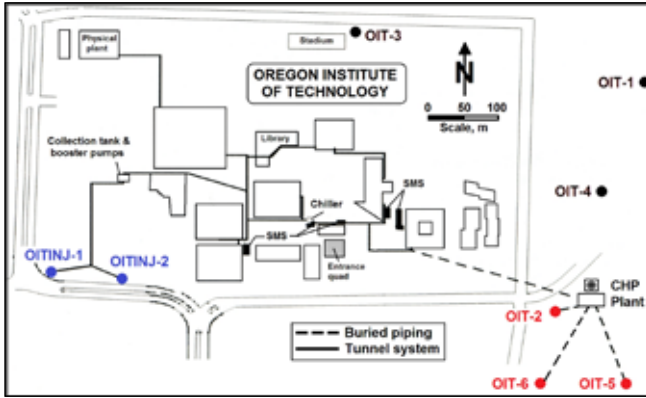


Figure 3. Layout of the campus of OIT and the locations of the production (red) and injection wells (blue): wells OIT-1 and -4 are used for domestic water, irrigation and cooling tower makeup; OIT-3 is not in use; SMS=Snow-Melt System; scale is approximate; modified and updated from Boyd, 1999.

Table 1. Selected characteristics of active OIT wells.

| Well No. | Production wells | | | Injection wells | |
|-----------------------------|------------------|------------------|------------------|------------------|--------------------|
| | OIT-2 | OIT-5 | OIT-6 | OITINJ-1 | OITINJ-2 |
| Total depth | 1,288 ft (393 m) | 1,716 ft (523 m) | 1,800 ft (549 m) | 2,005 ft (611 m) | 1,675 ft (511 m) |
| Depth to static water level | 332 ft (101 m) | 358 ft (109 m) | 359 ft (109 m) | 234 ft (71 m) | 173 ft (53 ft) |
| Volumetric flow rate | 150 GPM (9 L/s) | 460 GPM (29 L/s) | 350 GPM (22 L/s) | 400 GPM (25 L/s) | 1,000 GPM (63 L/s) |
| Pump mfr. | Goulds | Goulds | Layne/Bowler | N.A. | N.A. |
| Power | 50 hp (37.3 kW) | 75 hp (55.9 kW) | 75 hp (55.9 kW) | N.A. | N.A. |
| Pump setting depth | 700 ft (213 m) | 440 ft (134 m) | 600 ft (183 m) | N.A. | N.A. |
| Wellhead temperature | 192°F (89°C) | 195°F (91°C) | 197°F (92°C) | 98°F(1) (37°C) | 80°F(1) (27°C) |

(1) Original produced fluid.

POWER PLANT DESIGN

The OIT combined-heat-power plant is comprised of one modular organic Rankine cycle (ORC), a water cooling tower, and individual heat exchangers in various campus buildings. Three wells are available to send hot geofluid to the plant, although only two wells were in operation on the day the data were taken on which this paper is based. The power house and cooling tower are shown in Figure 4 and in simplified form, in the flow diagram depicted in Figure 5.



Figure 4. Power house with water cooling tower (Boyd and Lund, 2011).

The ORC was manufactured and supplied by Pratt & Whitney Power Systems and is called a Model 280 PureCycle® (UTC Power, 2008). Figure 6 is a site photo and Figure 7 is 3-D schematic rendering. Some characteristics of the unit are given in Table 2.

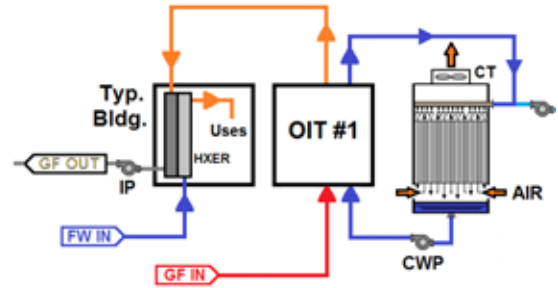


Figure 5. Overall system schematic flow diagram.

Table 2. Selected characteristics of PureCycle® unit.

| Item, units | Value |
|-----------------------------------|--------------------|
| Working fluid | R245fa(1) |
| Maximum rated gross power, kW | 280(2) |
| Maximum rated net power, kW | 260(3) |
| Turbine type | Radial inflow |
| Generator type | Induction |
| Power factor (lagging) | >0.95 |
| Noise (at 33 ft), dBA | 78 |
| Dimensions (L x W x H), ft | 19.9 x 7.5 x 11.25 |
| Operating weight, lbm | 33,300 |
| Inlet fluid temperature range, °F | 195-300 |

(1) 1,1,1,3,3-pentafluoropropane; (2) At 480 V/3-phase/60 Hz; (3) At 60 Hz.



Figure 6. ORC power module photo (Boyd and Lund, 201).

COMBINED HEAT-POWER PLANT OVERALL PERFORMANCE

The performance of the OIT Unit 1 power plant will be analyzed using the data obtained during a snapshot taken on January 20, 2012; see Figure 8. The relevant data for the geofluid and the cooling water are shown in Table 3; specific

volume, enthalpy and entropy values were found using REFPROP software (NIST, 2010). The net power of the ORC is used on site to run the well pumps, while the rest of the power is delivered to the campus. These data were obtained from another screen of the METASYS monitoring system, and the values are shown in Table 4. Although not shown in the screen shots, the geofluid temperature after leaving the heating system and entering the reinjection wells is 135°F.

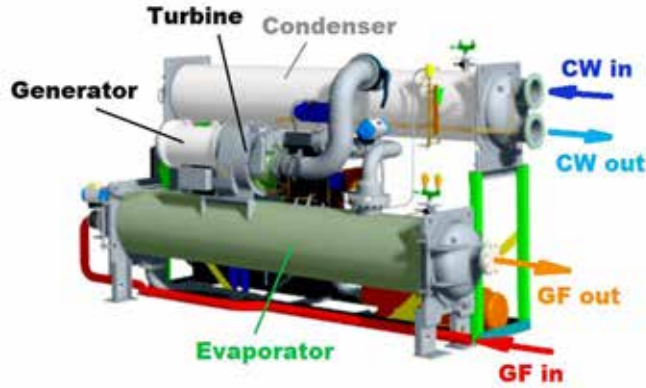


Figure 7. Power module schematic; feedpump and motor are located at ground level behind evaporator; control panel is at left rear (not visible).

Table 3. State-point properties for geofluid and cooling water; see Figures 8 and 10.

| State | Temp. (°F) | Pressure (psia) | Volume flow (GPM) | Specific volume (ft ³ /lbm) | Enthalpy (Btu/lbm) | Entropy (Btu/lbm.R) |
|---------------|------------|-----------------|-------------------|--|--------------------|---------------------|
| Geofluid | | | | | | |
| 1 | 196.9 | 26.72 | 624.3 | 0.01661222 | 165.16 | 0.28953 |
| 2 (1) | NA | NA | 624.3 | --- | TBD | TBD |
| 3 | 163.0 | 15.56 | 624.3 | --- | 131.11 | 0.23635 |
| 0 | 37.2 (wb) | 12.34 | --- | --- | 5.2575 | 0.010563 |
| Cooling water | | | | | | |
| 4 | 56.3 | 30 | 1,309 | 0.016029 | 24.477 | 0.048415 |
| 5 (1) | NA | NA | 1,309 | --- | TBD | TBD |
| 6 | 69.8 | 15 | 1,309 | --- | 37.942 | 0.074261 |

(1) Pinch-points.

Table 4. Power generation and usage.

| Item, units | Value |
|----------------------------|-------|
| Net cycle power, kW | 225.9 |
| Well-pumping power, kW | 148.0 |
| Power delivered to OIT, kW | 77.9 |

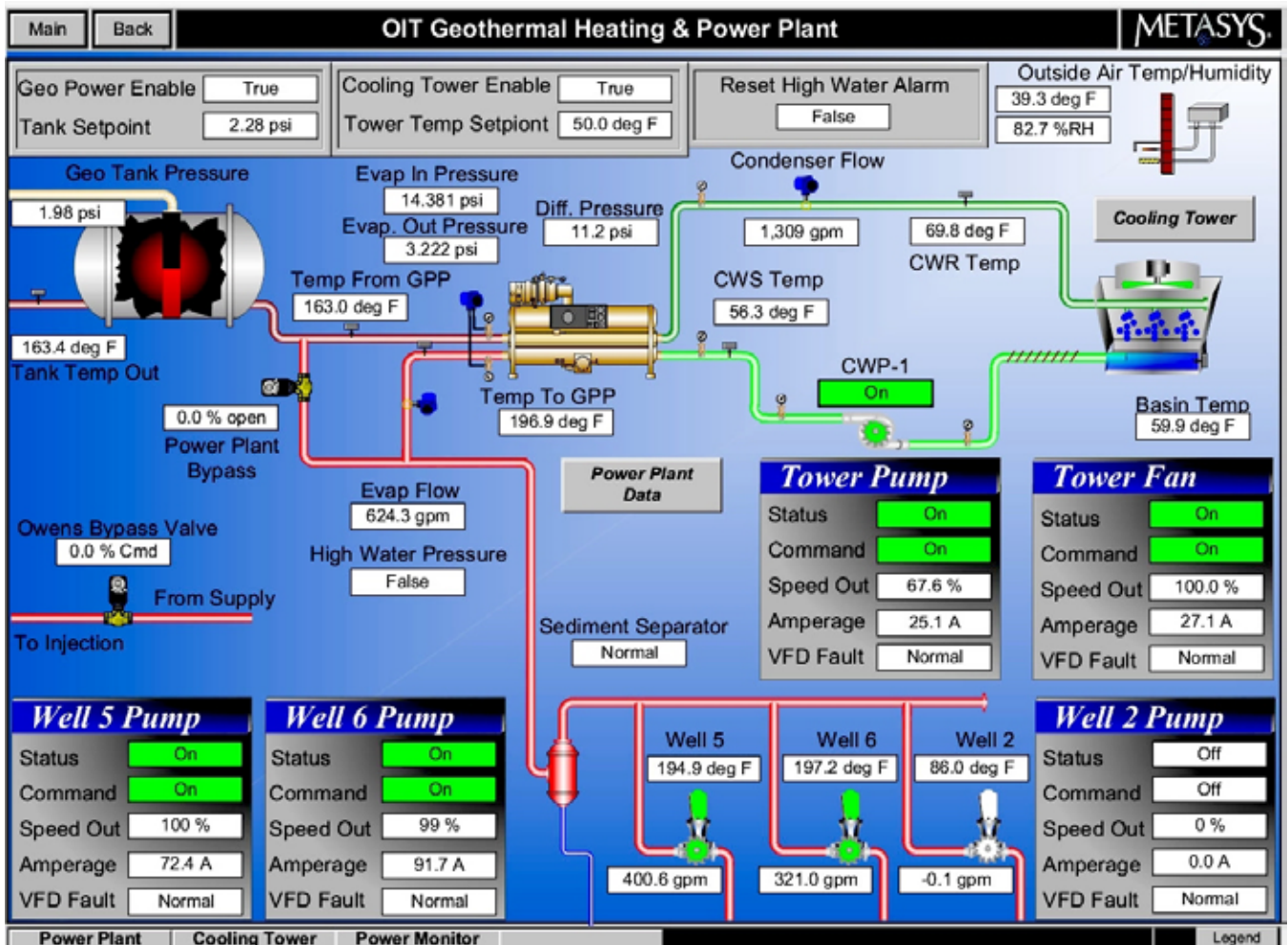


Figure 8. Screen shot of system flow diagram, January 20, 2012.

The goal of this section is to determine the thermal and utilization efficiencies of the plant. Although data for the geofluid and the cooling water are known, nothing is known about the thermodynamic state properties of the R245fa within the ORC since the manufacturer holds this information as proprietary. Thus, the overall performance is easy to calculate, but the detailed performance assessment of the cycle is not straightforward and will require several assumptions.

Figure 9 is a block diagram for the cyclic power unit (ORC) and its heat source and sink. Figure 10 is a more detailed representation of the plant, albeit still simplified.

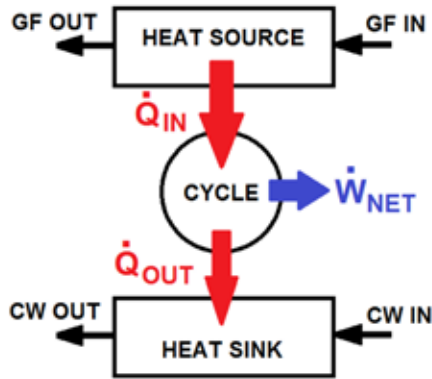


Figure 9. Simple overall system schematic.

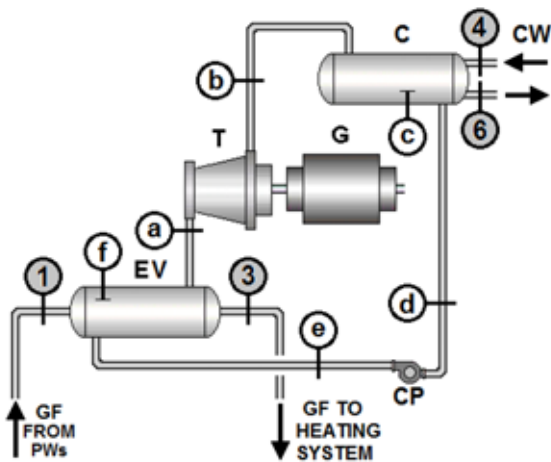


Figure 10. Simplified PureCycle® plant schematic flow diagram for OIT Unit 1.

The power cycle consists of the usual processes used in binary power plants:

- a-b: turbine expansion (power generation)
- a-bs: ideal isentropic turbine expansion (theoretical process)
- b-c: desuperheat removed in condenser
- c-d: Heat of condensation removed in condenser
- d-e: pressurization of liquid in feed pump
- d-es: ideal isentropic pressurization (theoretical process)
- e-f: sensible heat received in evaporator (preheating)
- f-a: latent heat received in evaporator (boiling).

The preheating (sensible heat) and the boiling (evaporation) both take place within a single shell-and-tube heat exchanger that is called the “evaporator”, EV. The geofluid enters the evaporator at one end and makes three passes, leaving at the opposite end. The R245fa enters at the bottom, flows through a series of baffled spaces within the shell, and leaves as a saturated vapor (assumed) at the top. Similarly, the desuperheating of the R245fa coming from the turbine takes place within a single shell-and-tube heat exchanger (the “condenser”, C) that also does the job of condensing the working fluid. The cooling water from the cooling tower enters and leaves at one end of the condenser shell, making four passes inside. The R245fa enters at the top and leaves at the bottom as a saturated liquid (assumed).

If the operation were ideal in the sense that all the heat removed from the geofluid (heat source) was actually transferred to the cycle working fluid, R245fa, and all the heat rejected by the R245fa actually ended up in the cooling water (heat sink), as shown in Figure 9, then the plant performance could be easily determined from the data given for the geofluid and the cooling water.

With reference to Figure 9, using basic thermodynamics:

$$Q_{IN} - Q_{OUT} = W_{NET} \quad (1)$$

Using the state-point notation in Figure 10:

$$Q_{IN} = m_{GF} (h_{IN} - h_{OUT})_{GF} = (V_{GF}/v_{GF,1})(h_1 - h_3) \quad (2)$$

and:

$$Q_{OUT} = m_{CW} (h_{OUT} - h_{IN})_{CW} = (V_{CW}/v_{CW,4})(h_6 - h_4) \quad (3)$$

Note that in the flow diagram Figure 10, we have reserved the state points 2 and 5 for the respective pinch-points of the geofluid and cooling water with the R245fa.

The mass flow rate of geofluid is found from the inlet conditions:

$$m_{GF} = V_{GF}/v_{GF,1} = (624.3 \times 0.13366 \times 60) / 0.01661222 = 301,382.2 \text{ lbm/h.} \quad (4)$$

The mass flow rate of cooling water is found similarly:

$$m_{CW} = V_{CW}/v_{GF,4} = (1,309 \times 0.13366 \times 60) / 0.01603019 = 654,867.8 \text{ lbm/h.} \quad (5)$$

Thus, the heat removed from the geofluid and the heat absorbed by the cooling water are, respectively:

$$Q_{IN} = 301,382.8 \times (165.16 - 131.11) / 3412 = 3,007.17 \text{ kW} \quad (6)$$

and:

$$Q_{OUT} = 654,867.8 \times (37.942 - 24.477) / 3412 = 2,534.17 \text{ kW} \quad (7)$$

Thus, without any heat losses, the expected net cycle power would be:

$$W_{NET} = 3,007.17 - 2,534.17 = 473.0 \text{ kW.} \quad (8)$$

However, the actual net power registered by the control system is only 225.9 kW and so, unsurprisingly, the system is non-ideal. Thus, equation (1) cannot be used to gauge the

system performance when the heat values are found from the geofluid and cooling water data. The basic equation, however, still applies to the R245fa cycle:

$$Q_{IN,Wf} - Q_{OUT,Wf} = W_{NET} = 225.9 \text{ kW.} \quad (9)$$

Clearly, $Q_{IN,Wf} \leq 3,007.17 \text{ kW}$ and/or $Q_{OUT,Wf} \geq 2,534.17 \text{ kW}$. In other words, either not all of the heat released from the geofluid ends up in the R245fa in the evaporator, or more heat is released by the R245fa in the condenser than is received by the cooling water, or both. Since the geofluid is the hottest fluid in the system, any imperfections in the insulation of the geofluid piping and evaporator covering would make it more likely that the former is true. Given the lower temperatures involved at the cold end of the plant, it is likely that the heat loss there is less than at the hot end. This will be used later to help understand the performance of the ORC unit.

Regardless of the non-ideality of the system, the overall thermal efficiency of the power plant can nevertheless be calculated:

$$\eta_{TH} = W_{NET}/Q_{IN,GF} = 225.9/3,007.17 = 0.0751 \text{ or } 7.51\% \quad (10)$$

The actual thermal efficiency of the ORC cycle itself will be somewhat higher than this.

The Second Law utilization efficiency can be found relative to the flow of exergy into the plant:

$$\eta_{U1} = W_{NET}/E_{GF,1} \quad (11)$$

where the incoming exergy is given by:

$$E_{GF,1} = m_{GF,1} [h_1 - h_0 - T_0(s_1 - s_0)] \quad (12)$$

$$= 301,382.8 [165.16 - 5.2575 - (37.2 + 459.67)(0.28953 - 0.010563)] / 3412 = 1,880.7 \text{ kW} \quad (13)$$

The thermodynamic dead state has been taken at the wet-bulb temperature (37.2°F) for the ambient conditions at the plant site and at the standard atmospheric pressure (12.34 psia) for the elevation of the plant (4,429 ft asl).

Thus,

$$\eta_{U1} = 225.9 / 1,88.7 = 0.120 \text{ or } 12.0\% \quad (14)$$

We may also calculate a utilization efficiency relative to the change in exergy of the geofluid as it passes through the unit:

$$\eta_{U2} = W_{NET} / \Delta E_{GF} \quad (15)$$

$$\Delta E_{GF} = m_{GF,1} [h_1 - h_3 - T_0(s_1 - s_3)] \quad (16)$$

$$= 301,382.8 [165.16 - 131.11 - (37.2 + 459.67)(0.28953 - 0.23635)] / 3412 = 673.65 \text{ kW} \quad (17)$$

$$\eta_{U2} = 225.9 / 673.65 = 0.3353 \text{ or } 33.53\% \quad (18)$$

The heating applications supplied by the geofluid after leaving the power plant may be lumped together and added to the useful output of the ORC to assess the full performance of the combined heat and power plant. Knowing the temperatures in and out of the heating system and the geofluid flow rate, the thermal power delivered from the geofluid may

be calculated from Equation (2) written between 163.4 and 135°F where a heat transfer efficiency of 90% is assumed between the geofluid and the secondary water in the building heat exchangers:

$$Q_{HTG} = 0.9 \times m_{GF}(h_{HTG,IN} - h_{HTG,OUT})_{GF} \\ = 0.9 \times (V_{GF}/v_{GF,IN})(h_{HTG,IN} - h_{HTG,OUT}) \quad (19)$$

$$Q_{HTG} = [(0.9 \times 624.3 \times 0.13366 \times 60) / 0.016412] (131.51 - 103.08) / 3412 = 2,287.7 \text{ kWt} \quad (20)$$

Thus, 2,287.7 kWt of direct heating can be attributed to the CHP plant. Thus, the total energetic benefit of the plant is $225.9 + 2,287.7 = 2,513.6 \text{ kW}$. The overall thermal efficiency becomes:

$$h_{TH, CHP} = (W_{NET} + Q_{HTG}) / Q_{IN,GF} = 2,513.6 / 3,007.17 \\ = 0.836 \text{ or } 83.6\% \quad (21)$$

ORC PERFORMANCE

Returning now to the problem of determining the performance of the ORC unit, an attempt will be made to thermodynamically fit the ORC between the geofluid cooling curve and the cooling water warming curve. This cannot be done precisely (or uniquely) because no data is available from the ORC manufacturer except the working fluid, R245fa. However, by assuming reasonable values for a set of parameters, it will be possible to arrive at a plausible ORC cycle.

Figures 11 and 12 show the temperature-heat transfer diagrams for the “evaporator” and “condenser”, respectively, in schematic form. Note that the “evaporator” incorporates both preheating and evaporation, and the “condenser” incorporates both desuperheating and condensation. In Figure 11, by postulating the R245fa evaporating pressure and the pinch-point temperature difference, $\Delta T_{PP,EV}$, and knowing the geofluid temperatures and flow rate, the First Law energy balance may be applied to the evaporator to determine the R245fa mass flow rate. A similar exercise on the condenser, using its pinch-point temperature difference, $\Delta T_{PP,C}$, will also yield the R245fa mass flow rate. It is not expected that the two values will be equal owing to the heat losses mentioned earlier and some means must be found to account for this situation.

Simultaneously, the ORC turbine power, pump power and generator output can be calculated with the aid of chosen isentropic efficiencies for the turbine and pump and a generator mechanical-to-electrical conversion efficiency. Thus, a multi-variable search must be carried out until the net ORC power agrees with (or compares very well) with the measured value. The following parameters need to be adjusted while searching for a reasonable answer:

R245fa evaporator pressure ($P_e = P_f = P_a$)

R245fa condenser pressure ($P_b = P_c = P_d$)

Evaporator pinch-point temperature difference, $\Delta T_{PP,EV}$

Condenser pinch-point temperature difference, $\Delta T_{PP,C}$

R245fa turbine isentropic efficiency, η_T

R245fa pump isentropic efficiency, η_P .

The generator efficiency, η_G , was set at 0.95 (95%) and kept constant.

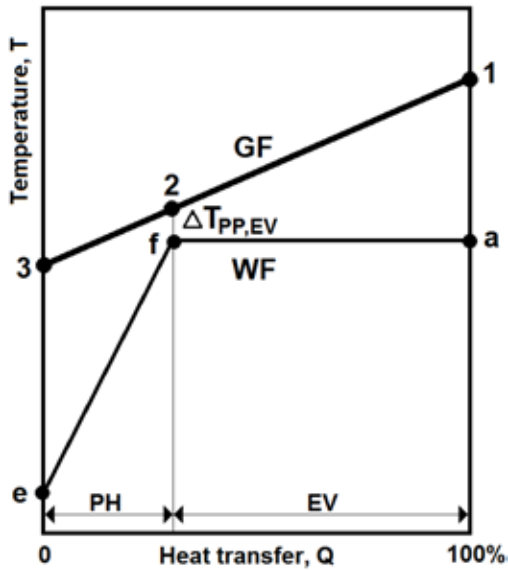


Figure 11. Temperature-heat transfer diagram for “evaporator”.

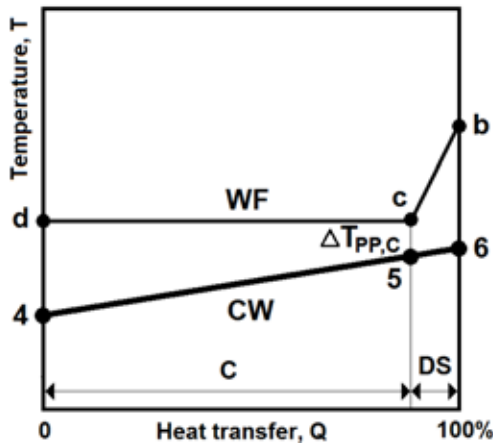


Figure 12. Temperature-heat transfer diagram for “condenser”.

An Excel spreadsheet was written to perform the calculations and REFPROP was embedded in it to obtain all thermodynamic properties for the geofluid (assumed pure water), the cooling water, and the R245fa.

The method of solution is as follows. The pinch-points were taken at the bubble point in the evaporator and at the dew point in the condenser. The locations of these points along the GF and CW curves were assumed as a first guess; i.e., at a certain percentage of the total heat transfer in each heat exchanger; see Figures 11 and 12. Thus, the temperature was found on the GF and CW lines at the pinch-points. Using assumed values for the ΔT_{PP} -terms, the saturation temperatures for the R245fa in the evaporator and in the condenser were found. The heat transfer terms in the evaporator and condenser were calculated along with the matching R245fa mass flow rates. Then the percentage of heat transfer to each pinch-point was calculated and compared to the earlier assumed values. Adjustments were successively

made until agreement was obtained. The power terms were also found at each iteration and compared to the measured value of net ORC power. Eventually, the calculations converged to yield a net power of 225.9 kW, but as expected, the mass flow rates of R245fa calculated for each heat exchanger differed significantly, being about 10% apart, and this solution was deemed unacceptable.

In order to simulate the apparent heat loss between the geofluid and the R245fa, the heuristic assumption was made that only 92% of the heat removed from the geofluid was effectively delivered to the R245fa; i.e., there is an 8% heat loss. Additionally, no loss was ascribed to the heat transfer at the condenser end of the plant. Closure was achieved on the iterative solution using the following values for system parameters:

$$\text{R245fa evaporator pressure } (P_e = P_f = P_a) = 85.25 \text{ psia}$$

$$\text{R245fa condenser pressure } (P_b = P_c = P_d) = 24.86 \text{ psia}$$

$$\text{Evaporator pinch-point temperature difference, } \Delta T_{PP,EV} = 16^\circ\text{F}$$

$$\text{Condenser pinch-point temperature difference, } \Delta T_{PP,C} = 15^\circ\text{F}$$

$$\text{R245fa turbine isentropic efficiency, } \eta_T = 0.85$$

$$\text{R245fa pump isentropic efficiency, } \eta_P = 0.75.$$

The final results for the state-point properties of the R245fa in the ORC are shown in Table 5. The mass flow rates now differ by only $\pm 0.2\%$, an acceptable amount given the level of uncertainty inherent in the analysis. The R245fa mass flow rate through the evaporator was calculated from:

$$m_{R,EV} = m_{GF} [0.92(h_1 - h_3)/(h_a - h_e)] \quad (22)$$

and through the condenser from:

$$m_{R,C} = m_{CW} (h_6 - h_4)/(h_b - h_d) \quad (23)$$

Table 5. State-point properties for ORC working fluid R245fa.

| State | Temp. (°F) | Pressure (psia) | Enthalpy (Btu/lbm) | Entropy (Btu/lbm.R) | Mass Flow (lbm/h) |
|---------------------------------|------------|-----------------|--------------------|---------------------|------------------------|
| Steam & condensate state-points | | | | | |
| a | 155.54 | 85.24 | 195.34 | 0.42371 | 101,630 ⁽¹⁾ |
| bs | --- | 24.86 | 185.73 | 0.42371 | --- |
| b | 101.65 | 24.86 | 187.17 | 0.42630 | 101,850 ⁽²⁾ |
| c | 84.16 | 24.86 | 183.13 | 0.41899 | 101,850 ⁽²⁾ |
| d | 84.16 | 24.86 | 102.28 | 0.27031 | 101,850 ⁽²⁾ |
| es | --- | 85.24 | 102.41 | 0.27031 | --- |
| e | 84.57 | 85.24 | 102.46 | 0.27039 | 101,630 ⁽¹⁾ |
| f | 155.54 | 85.24 | 125.89 | 0.31082 | 101,630 ⁽¹⁾ |

Obtained from Eq. (19); (2) Obtained from Eq. (20).

The turbine and pump power were calculated using the average of these two mass flow rates. The net ORC power under these conditions is 226.0 kW, only 0.1 kW higher than the measured power, or 0.04% error which is probably less

than the accuracy of the instrumentation. However, it must be stressed that this solution is not unique as there may be other combinations of the system parameters that might give equivalent results. The cycle processes are shown to scale in Figure 13, a temperature-entropy diagram.

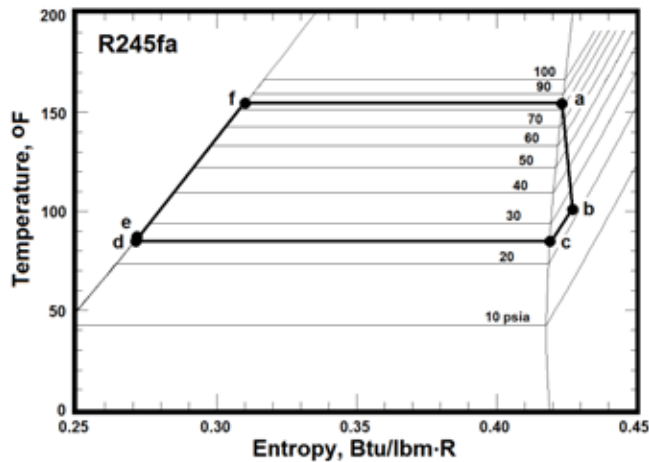


Figure 13. R245fa processes for OIT unit in temperature-entropy coordinates.

The heat and work transfer terms were found from the standard thermodynamic equations. Cycle and plant efficiencies were computed using the First and Second Laws of thermodynamics. Table 6 shows the results for the ORC cycle.

Table 6. Calculated ORC cycle results for state-points given in Table 5.

| Item, units | Value |
|---------------------------------|---------|
| Evaporator heat duty, kWt | 2,766.6 |
| Specific turbine power, Btu/lbm | 8.167 |
| Gross turbine power, kW | 243.53 |
| Generator gross output, kW | 231.35 |
| Condenser heat duty, kWt | 2,534.2 |
| Specific pump power, Btu/lbm | 0.1798 |
| Pump power, kW | 5.361 |
| Generator net output, kW | 226.0 |
| Thermal efficiency, % | 8.2 |

CONCLUSION

The OIT CHP plant serves both as an educational opportunity for students and as an economic, green means of providing heat and electricity to the campus. In light of the relatively low temperature of the geofluid entering the plant, the efficiencies based on energy and exergy are quite reasonable. Accounting for both heat delivered to the campus buildings and electricity generated, the CHP plant is about 84% efficient in terms of the heat delivered by the incoming geofluid. Since the plant allows OIT to avoid buying electricity from the regional supplier, Pacific Power, this means an avoidance of carbon dioxide emissions in proportion to the generation mix by Pacific Power that includes 79% from fossil fuels, coal and natural gas combined. The plant requires no human supervision and basically runs itself. One operating problem involved the cooling tower freezing up on the external surface but that has been taken care of by the facilities personnel.

EDITOR'S NOTE

This paper was originally published in the Geothermal Resources Council Transactions, Volume 36, Geothermal: Reliable, Renewable, Global, GRC 2012 Annual Meeting and reprinted with permission from the Geothermal Resources Council and authors.

REFERENCES

- Boyd, T.L., "The Oregon Institute of Technology Geothermal Heating System – Then and Now," *Geo-Heat Center Quarterly Bulletin*, V. 20, No. 1, March 1999, pp. 10-13.
- Boyd, T. and J.W. Lund, "Trials and Tribulation of the Oregon Institute of Technology Small-Scale Power Plant," *Geo-Heat Center Quarterly Bulletin*, V. 30, No. 2, August 2011, pp. 6-9.
- UTC Power, 2008. "Model 280 PureCycle System", Factsheet, UTC Power, A United Technologies Company, 2 p.
- National Institute of Standards and Technology, 2010. "NIST Reference Fluid Thermodynamic and Transport Properties Database (REFPROP): Version 9.0", National Institute of Standards and Technology, U.S. Department of Commerce <http://www.nist.gov/srd/nist23.cfm>.

CONCENTRATED SOLAR AND GEOTHERMAL HYBRID POWER PROJECT

*Guy Nelson, Utility Energy Forum, Lincoln City, Oregon
Garth Larsen, PacifiCorp*

ABSTRACT

There is an opportunity to add a concentrated solar power (CSP) system to an existing geothermal power plant. The addition of the CSP system would create a hybrid project that maintains or improves the power output of the geothermal power plant facility.

If viable, this opportunity is important because the marriage of two or more renewable energy technologies can optimize resources and support the following concepts:

- promote the energy park concept,
- increase the cost-effectiveness of developing utility scale renewable technologies,
- support the goals and objectives of the Western Governors' Association - Renewable Energy Zone (REZ), and
- encourage geothermal and solar stakeholder collaboration.

CSP systems use mirrors or lenses to concentrate a large area of sunlight onto a small area. In CSP stand alone projects, electrical power is produced when the concentrated light is converted to heat, which drives a heat engine (usually a steam turbine) connected to an electrical power generator. In a CSP/Geothermal hybrid project the heat would be used to heat the spent brine or another working fluid.

This paper describes a variety of potential hybrid projects and includes discussions on (1) CSP technologies, (2) hybrid project scenarios, (3) hybrid project cost and benefits, and (4) next steps. Although the paper focuses on hybrid project application to existing and future hydrothermal power plants, hybrid projects could have potential in enhanced geothermal systems.

CSP TECHNOLOGIES

According to the Interstate Renewable Energy Council (IREC), CSP is being widely commercialized and the CSP market has seen about 740 MW of generating capacity added between 2007 and the end of 2010. More than half of this (about 478 MW) was installed during 2010, bringing the global total to 1,095 MW. The US ended the year with 509 MW after adding 78 MW, including two fossil-CSP hybrid plants (Sherwood, 2010).

CSP technologies exist in four common forms, namely parabolic trough, dish Stirling, concentrating linear Fresnel reflector, and solar power tower. CSP is used to produce electricity, sometimes called solar thermoelectricity, usually generated through steam. Concentrated-solar technology systems use mirrors or lenses with tracking systems to focus a large area of sunlight onto a small area. The concentrated light is then used as heat or as a heat source for a conventional power plant. The solar concentrators used in CSP systems

can often also be used to provide industrial process heating or cooling, such as in solar air-conditioning.

A parabolic trough consists of a linear parabolic reflector that concentrates light onto a receiver positioned along the reflector's focal line. The receiver is a tube positioned directly above the middle of the parabolic mirror and filled with a working fluid. The reflector follows the sun during the daylight hours by tracking along a single axis. A working fluid such as molten salt is heated to 150–350°C as it flows through the receiver and is then used as a heat source for a power generation system.

Fresnel reflectors are made of many thin, flat mirror strips to concentrate sunlight onto tubes through which working fluid is pumped. Flat mirrors allow more reflective surface in the same amount of space as a parabolic reflector, thus capturing more of the available sunlight, and they are much cheaper than parabolic reflectors. Fresnel reflectors can be used in various size CSPs.

A dish Stirling or dish engine system consists of a stand-alone parabolic reflector that concentrates light onto a receiver positioned at the reflector's focal point. The reflector tracks the Sun along two axes. The working fluid in the receiver is heated to 250–700°C and then used by a Stirling engine to generate power. Parabolic-dish systems provide the highest solar-to-electric efficiency among CSP technologies, and their modular nature provides scalability.

A solar power tower consists of an array of dual-axis tracking reflectors that concentrate light on a central receiver atop a tower; the receiver contains a fluid deposit, which can consist of sea water. The working fluid in the receiver is heated to 500–1000°C and then used as a heat source for a power generation or energy storage system.

HYBRID PROJECT SCENARIOS

CSP/Geothermal hybrid projects could be a number of scenarios, all of which use the heat generated by the CSP system to enhance the geothermal project.

1. In steam or flash geothermal power plants, the CSP system could reheat the spent brine, either directly or through a working fluid tied to a heat exchanger, and allow all or a portion of the brine to be recycled back into the geothermal plant to pass through another flash tank and reintroduced to the steam turbine and/or re-injected into the reservoir at a higher temperature.
2. In binary power plants, the CSP system could reheat the spent brine (again, either directly or via a working fluid) and allow all or a portion of the brine to be recycled back into the power plant and/or re-injected into the reservoir at a higher temperature. Re-injection at higher temperatures could off-set the need for the

expense and risk exposure experienced when using acid for brine pH modification. Potentially, the higher reinjection temperature will retard the rate of silica polymerization.

3. In binary power plants, the CSP system could heat the working fluid to a higher temperature to produce more power.
4. In binary and flash units, CSP systems could be utilized to off-set parasitic load. The use of CSP would not require additional inter-connection costs as it would be used for plant consumption thus allowing the geothermal net electrical production to increase by the CSP off-set.

In all of the above scenarios, the hybrid project reduces the stress on the reservoir by either producing more power and/or increasing the temperature of the re-injected brine. Increasing the temperature of the re-injected brine increases the temperature/pressure thermodynamics of the reservoir. The hybrid technology can also apply to future enhanced geothermal systems. A simplified CSP flow diagram is shown in Figure 1.

COSTS AND BENEFITS

As of September 2009, the cost of building a stand-alone CSP station was typically about \$2.50 to \$4.00 per watt. Given that cost, the energy cost from a 250 MW CSP station

would be \$0.12 to \$0.18/kWh. The cost range is based on information in a November 2008 Congressional Research Service report to Congress (Kaplan, 2008). The report analyzed four major factors that determine the cost of electricity from new power plants:

1. construction costs,
2. fuel expense,
3. environmental regulations, and
4. financing costs.

Although the report is four years old, there may not be a better document that provides projections of the possible cost of power from new fossil, nuclear, and renewable plants or that describes how different assumptions, such as for the availability of federal incentives, change the cost rankings of the technologies.

There is evidence that the costs will drop in the future. For example, in 2009, National Renewable Energy Laboratory (NREL) and SkyFuel staff teamed to develop large curved sheets of metal that have the potential to be 30% less expensive than today's best collectors of concentrated solar power by replacing glass-based models with a silver polymer sheet that has the same performance as the heavy glass mirrors, but at much lower cost and weight. It also is much easier to deploy and install. The glossy film uses several layers of polymers, with an inner layer of pure silver.

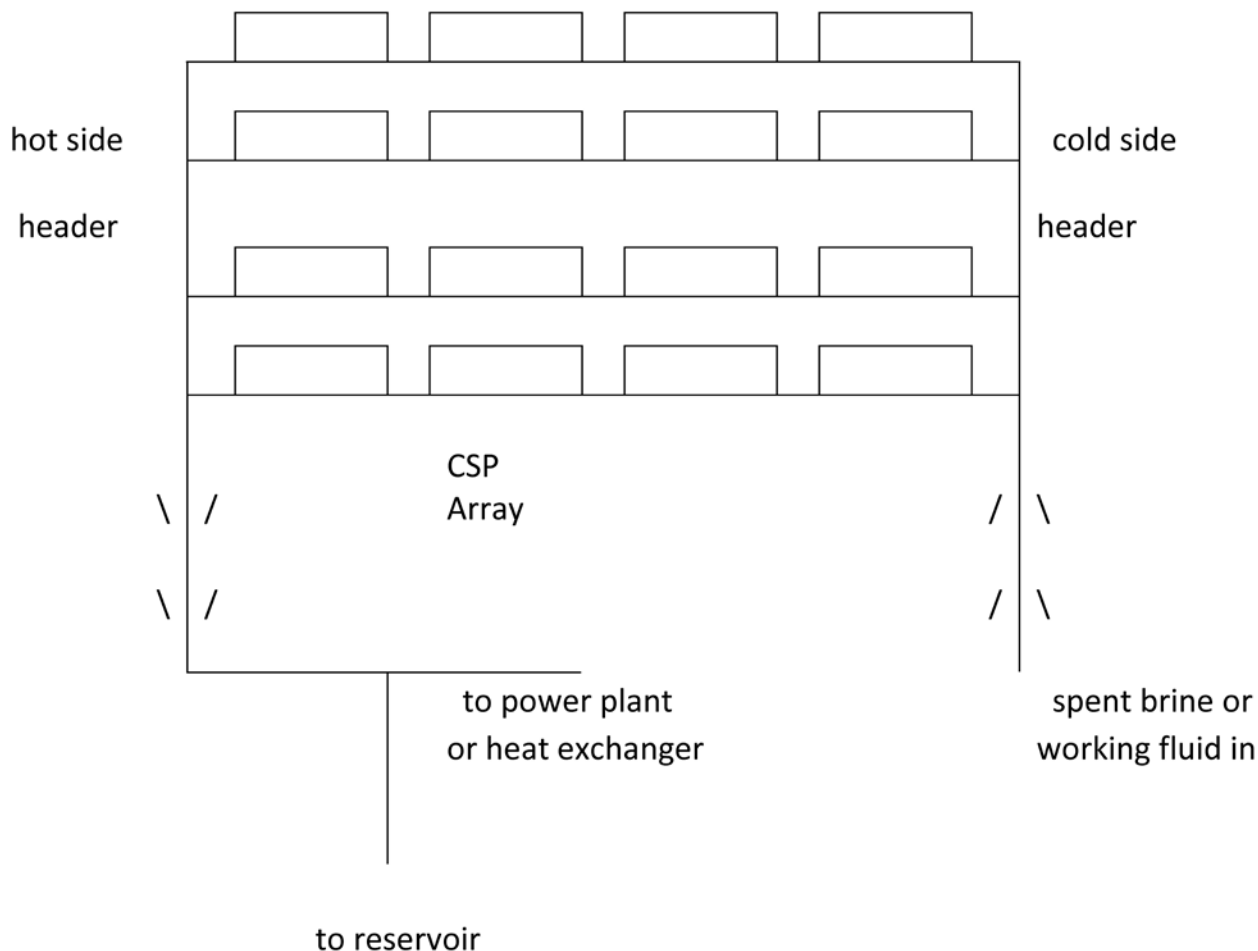


Figure 1. Simplified CSP Flow Diagram.

The economics of a hybrid CSP/Geothermal project will likely be more attractive than the CSP stand-alone project, because of less storage requirements. Also, the integration into the existing geothermal power plant infrastructure can lower CSP costs. Furthermore, CSP works best with areas of high solar radiation, such as the southwest United States. This area is also where there are existing geothermal power plants and where there is significant geothermal potential.

CSP can contribute to the long-term success and profitability of a geothermal project by extending the life of the geothermal reservoir and reducing the need to drill additional production wells or relocating injection wells. Drilling costs for new wells can be \$5 million or higher, depending on geologic conditions and depth requirements. CSP can also contribute to the benefit of using dry cooling towers in arid climates. CSP can offset parasitic load, thus making more megawatts available to the market and mitigating the negative impact of reduced output during summer peak due to high ambient temperatures. This can especially be applied in dry climates where water is scarce and the need to conserve water is significant. Thus, supplementing the parasitic load with CSP can reduce costs of buying and treating water and can also significantly reduce the rate of reservoir depletion due to evaporative loss. Augmenting parasitic load with CSP can effectively extend the life of the geothermal reservoir and improve the long-term economics of the geothermal project.

Like oil and gas reservoirs, geothermal reservoirs can reduce output if not properly managed. For example, overproduction of a reservoir, such as was historically practiced in the Geysers geothermal field in northern California, leads to a significant shortening of its productive lifetime and a loss of income. Even a properly managed reservoir often requires relocation of production and reinjection wells to maintain an acceptable output. A hybrid project can delay or eliminate the need to drill new wells or redesign the reservoir gathering and re-injection system.

The hybrid application can also help get more CSP equipment installed in the U.S. According to an Emerging Energy Report, Spain has eclipsed the U.S. in CSP potential

and U.S. applications must compete with lowering power demand, energy prices, and PV module costs (Emerging Energy Research, 2010).

NEXT STEPS

The CSP/Geothermal hybrid project is only a concept at this time. The next steps to move the project from conception to implementation include

1. Identify potential hybrid project sites (month one).
2. Assess industry support (month two through three).
3. Refine cost and benefits (month two through four).
4. Determine Go/No Go Decision on developing a project. Several factors go into determining the Go/No Go Decision (Step 5), including confidence in the cost and benefits of the project and budget to fund one or more projects through project partnership funds, including potential grant awards

EDITOR'S NOTE

This paper was originally published in the Geothermal Resources Council Transactions, Volume 36, Geothermal: Reliable, Renewable, Global, GRC 2012 Annual Meeting and reprinted with permission from the Geothermal Resources Council and authors.

REFERENCES

- Sherwood, L., 2010. "U.S. Solar Market Trends", Interstate Renewable Energy Council, <http://irecusa.org/wp-content/uploads/2011/07/IREC-Solar-Market-Trends-Report-revised070811.pdf>
- Emerging Energy Research, 2010. "Global Concentrated Solar Power markets and Strategies: 2010-2025", Emerging Energy Research, <http://www.emerging-energy.com/uploadDocs/GlobalConcentratedSolarPowerMarketsandStrategies2010.pdf>
- Kaplan, S., 2008. "CRS Report for Congress - Power Plants: Characteristics and Costs", Congressional Research Service, <http://www.fas.org/sgp/crs/misc/RL34746.pdf>.

HYBRID GEOTHERMAL AND SOLAR THERMAL POWER PLANT CASE STUDY; GÜMÜŞKÖY GEPP

Ö. Çağlan Kuyumcu, Umut Z. D. Solaroğlu, Sertaç Akar, & Onur Serin, BM Holdings Inc., Ankara, Turkey

ABSTRACT

Performance of air cooled ORC geothermal power systems are inversely related with ambient temperature, where summer temperature extremes can cause performance drops of up to 70% from design. Concentrating Solar Thermal power generation systems act inversely, almost in harmony, reaching peak efficiency during most of these ambient temperature extremes. The two thermal generation systems constitute suitable candidates for hybridization, as a way of “hedging production against ambient temperature fluctuations”. BM Holdings is currently developing this concept in its Gümüşköy GEPP that is under construction, where the existing 6.6MWe geothermal power unit shall be complemented by a CSP system of adequate size in order to improve overall system efficiency while keeping a manageable Levelized Cost of Electricity (LCOE). A pilot solar field is planned to be erected in 2012 and full scale implementation is planned for 2013.

INTRODUCTION

The world's current levels of growing energy demands and global warming effects are forcing our global community to display an increasing effort in transitioning to renewable energy resources. On the other hand given the more expensive levelized cost of renewable electricity (LCOE), there is a strong demand for viable renewable energy projects.

Geothermal power is considered to be a sustainable renewable resource, because the heat extraction is negligibly small compared with the Earth's heat content and is constantly replenished by radioactive activity within the Earth. On the geothermal front, Turkey – being in a tectonically active zone – is the 7th in the world in geothermal potential, estimated at 2500 MWe and 31,500 MWt (Şimşek et. al, 2005). This potential is largely dormant, where according to Energy Market Regulations Authority (EMRA) 2012 data, the present installed geothermal power generation capacity in Turkey is 115 MWe, with 370 MWe more under development and construction (Serpen et. al, 2010; Mertoğlu et.al, 2010). On the other hand, this rate of growth is still slow, owing to a number of problems inherent in the technology and the share of geothermal in the total primary energy supply of Turkey is still below 1.5 % (Ediger & Akar, 2007).

Geothermal electric plants have until recently been built exclusively where high temperature geothermal resources were available near the surface. The development of binary cycle power plants and improvements in drilling and extraction technology helped extend geothermal power generation to lower temperature fields. However, thermal efficiency of geothermal electric plants is relatively low, around 10-23%. In accordance with the laws of thermodynamics, heat or energy (via pressure) extraction from lower temperatures still limits the efficiency of the process and increases LCOE from geothermal.

Since there is no fuel cost, this does not necessarily affect operational costs. However it necessitates very high flow rates of geothermal brine to supply the required enthalpy, which leads to a high number of wells and pump costs. Plant CAPEX is therefore increased. In comparison, fossil fuel based thermal power plants can heat steam to much greater temperatures than geothermal power can and therefore reach higher efficiencies.

Another factor increasing LCOE is ambient temperature. Geothermal plants lose a lot of efficiency when operating in off-design high temperatures, owing to reduced pressure difference between the turbine input and output during hot summer days. As a result, geothermal power is still in need of subsidies in order to survive and spread.

HYBRID POWER PLANT CONCEPT

Approach

Once current renewable energy generation technologies are investigated, a very interesting match is observed between solar thermal and geothermal energy. Solar energy refers to energy that comes directly from the sun's radiation. It is utilized in two main ways, which are photovoltaic devices and through thermal heat collections. Photovoltaic devices absorb photons from the sun, which directly excite a flow of electrons to generate electricity. Solar heat can be used for concentrated into a heat transfer fluid, which operates a thermodynamic cycle to convert heat into electricity (Greenhut, 2010). The latter solar energy generation method is also referred to as Concentrating Solar Power, or CSP.

Both solar thermal (CSP) and geothermal energy generation methods operate a thermodynamic cycle, by heating a working fluid (or water) that drives steam turbines. Therefore, the two energy generation methodologies differ in heat collection but share the same power island structure.

Additional synergy is found in the inverse relation between the two technologies' operational efficiencies with ambient temperature. Air-cooled Rankine cycle geothermal power plants lose a lot of efficiency when operating in off-design high temperatures, such as during summer and daytime ambient temperature peaks. The base geothermal plant can produce only 60% of its peak generation in July (Greenhut, 2010). Solar thermal technologies operate at peak efficiency at exactly these times when ambient temperature is highest and efficiency of geothermal plants is at their lowest.

A proposition for a hybrid geothermal and solar thermal energy conversion system for locations having both resources can therefore be formulated based on these synergies between them. The hybrid system would aim to integrate an adequate capacity of CSP (without heat regulation) to a regular geothermal power plant, which would add sufficient enthalpy to the thermodynamic system to cover (i.e. eliminate) high ambient

temperature related efficiency losses. Such a hybrid system would produce solar energy (equivalent to the value of added enthalpy), without additional power island investment, since this is already present in the geothermal system. The result would be a higher capacity renewable energy generation system with a more stable efficiency and good LCOE. Economic analyses already show that with respect to small size stand-alone ORC plants, much lower costs, up to 50% less, can be obtained with this technology (Astolfi et. al, 2011).

Availability of Resources at Target Location

Turkey has respectable solar radiation levels of up to 1980 kWh/m² in certain parts that can easily support solar thermal energy generation (Kaygusuz, 2011). More importantly, there are many parts of Turkey that have both strong solar radiation levels and geothermal resources (Figure 1).

The project location selected for this study is in Gümüşköy, Aydın, which was preferred for having both abundant geothermal resources suited to air-cooled ORC power generation as well as good levels of solar radiation (average 1311 kWh/m²) and suitable land for placing solar fields.

The Gümüşköy geothermal field produces from a 2000 m deep reservoir of approximately 180°C, with a production temperature of 165°C. Gümüşköy Geothermal Power Plant (GK GEPP) Stages I and II are currently under construction, which will comprise 6.6MWe power units each for a total of 13.2MWe installed power capacity.

The current hybridization study was based on Stage I of the project that operates 6.6MWe power with 432 ton/hour of brine.

Preferred Hybridization Configuration

Hybridization studies commenced with systems combining geothermal energy generation systems with fossil fuel based thermal systems for superheating (Kohl and Speck, 2004). Other studies considered base-load oriented three way hybrids of CSP, geothermal and fossil fuel based thermal systems (cascading closed loop cycle) and geothermal and biogas hybrids (Kreuter and Kapp, 2008).

Geothermal and solar thermal hybrid power plants may be built with binary cycle (ORC) or flash steam geothermal plants on the geothermal end, and in different configurations. An example of solar–geothermal integration for electricity generation was proposed for the Cerro Prieto field in Mexico (Lentz & Almanza, 2006). Another example of solar–geothermal integration for electricity generation was built for Stillwater field in Nevada.

There are multiple ways that may be chosen to build geothermal and CSP power generation hybrids. Some of the power cycle configurations that have been investigated in the past are as follows (Greenhut, 2010):

1. **Working fluid superheat concept:** This approach utilizes solar heat to raise the temperature of the working fluid in a geothermal power generation cycle before it enters the turbines, resulting in higher working fluid energy and power generation.
2. **Brine preheat concept:** This approach utilizes solar heat to raise the temperature of the geothermal brine before it enters the heat exchangers, resulting in higher brine enthalpy and thus higher power generation.
3. **Brine recirculation concept:** This approach utilizes solar heat to raise the temperature of a portion of the recirculating brine coming out of the heat exchangers to that of the fresh brine and add this recirculate brine into the feed to the heat exchangers. This results in a lower fresh brine requirement, thus higher power generation from the same field.
4. **Brine preheat/recirculation concept:** This approach utilizes solar heat to raise the temperature of both the geothermal brine before it enters the heat exchangers and also of a portion of the recirculating brine and feed this to the heat exchangers. This results in higher brine enthalpy as well as lower fresh brine requirement, thus higher power generation.
5. **Brine cascade reheat concept:** This approach utilizes solar heat to raise the temperature of the recirculating brine coming out of the heat exchanger to or above its



Figure 1. Solar radiation levels in Turkey (General Directorate of Electrical Power Survey Administration of Turkey)

original temperature and feed this to a second heat exchanger / power generation unit. This results in a much higher power generation from the same field.

Studies concluded that while the cascade reheat concept yields the highest solar utilization efficiency, the superheat and preheat systems produced the lowest incremental LCOE. A direct comparison between superheat and preheat systems suggests lower LCOE for the superheat concept, which eliminates thermodynamic losses in the heat exchangers.

Basis for Hybridization

The proposition for hybrid geothermal system and CSP in Gümüşköy GEPP are based on the following synergies that exist between them:

- **Availability of resources:** Geothermal reserves as well as strong solar radiation levels are available together in many locations in Turkey. One example is Gümüşköy in Aydın.
- **Maximizing operational efficiency:** Combining the two technologies enables CSP's operational peaks at high ambient temperatures compensate for the loss of efficiency in the geothermal system, thereby giving a combined overall efficiency that is higher than that of both systems.
- **Equipment sharing:** Both energy sources would share common equipment, such as turbines, condenser and heat exchangers. This allows joint use of the equipment for both solar thermal and geothermal generation.
- **Maximizing energy generation:** Using solar thermal energy to boost geothermal plant performance during the day, when solar radiation is at maximum, also helps realize the full energy generation of the installed power capacity. This enables higher renewable energy generation from the same geothermal field, which helps replace fossil fuel based generation.
- **Financial mitigation:** A hybrid system can mitigate the high cost of solar projects with the low cost of geothermal projects (Greenhut, 2010).
- **Ability to capture incentives:** Different economic incentives are available for different technologies. By combining geothermal and solar technology, hybrid systems can qualify for more forms of economic support (Greenhut, 2010).

CSP heat regulation systems have not been considered since in the classical sense, these are both extremely costly in comparison to the current considerations, as well as out of line with the synergy for maximizing operational efficiency. Partial regulation schemes through storage have not been addressed but may be assessed in a future study.

INDIVIDUAL SYSTEMS

Efficiency of ORC

When an air cooled condenser (ACC) is used as the plant's heat sink, then there exists a decline in net electricity generation of the turbines when ambient air temperature is high. At an extreme ambient temperature of 45°C, this loss of efficiency can reach up to 80% (Figure 2). The reverse is also

true, where a surplus occurs in energy efficiency during ambient temperatures below the optimum operating temperature.

The average brine temperature produced from the Gümüşköy Geothermal Field is 165°C, with 80°C return (re-injection) temperature. The plant design uses air-cooled condensers and therefore suffers a decrease in power generation during hot seasons owing to ambient temperature highs. Calculations show that the plant's power net production capacity drops from its maximum 7.3 MWe and design 6.6 MWe to as low as 3.9 MWe average for several months, depending on the ambient temperature (Figures 3 and 4). This corresponds to a total efficiency loss of up to 40%.

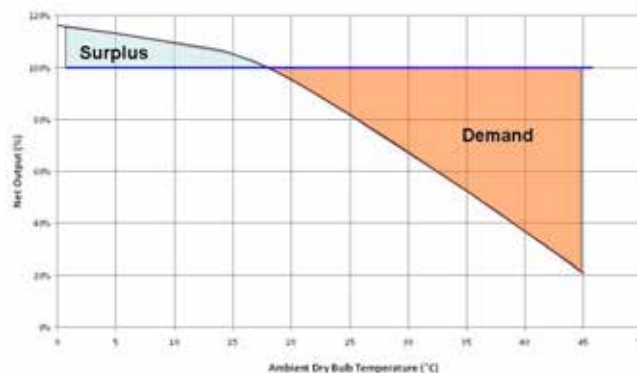


Figure 2. ACC ORC typical efficiency with respect to ambient dry bulb air temperature

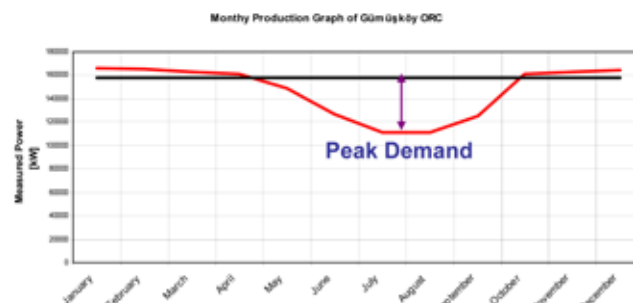


Figure 3. GK GEPP Stage I annual net power variation

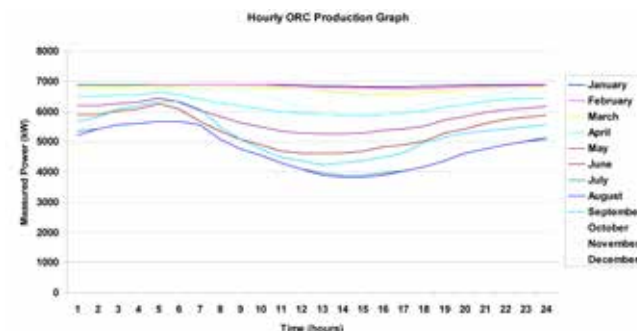


Figure 4. GK GEPP daily net power variation throughout the year

The initial objective is to build a solar field of adequate capacity in the adjacent land areas and utilize the enthalpy generated from the solar field to superheat the geothermal fluid to a temperature that would ensure 6.6 MWe (100%

design) or 7.3 MWe (peak generation) power generation through a much longer time period within the year. Naturally, the project economics must still consider shortcomings of the hybridization such as hot summer nights without solar radiation that would still lead to decreases in overall efficiency.

Efficiency of CSP

CSP systems are categorized as three different design alternatives: parabolic trough, power tower and dish/stirling which are basically solar thermal concentrating devices. Direct Normal Insolation (DNI) is reflected and concentrated onto a receiver or absorber where it is converted to heat, then the heat is used to produce steam to drive a traditional rankine power cycle. In Gümüşköy GEPP case study, parabolic trough collectors will be utilized. Parabolic trough system is line-focusing, and it uses the mirrored surface of a linear parabolic concentrator to focus direct solar radiation to an absorber pipe running along the focal line of the parabola. The heat transfer fluid (HTF) or water inside the absorber pipe is heated and pumped to the steam generator, which in turn is connected to a steam turbine to produce electricity.

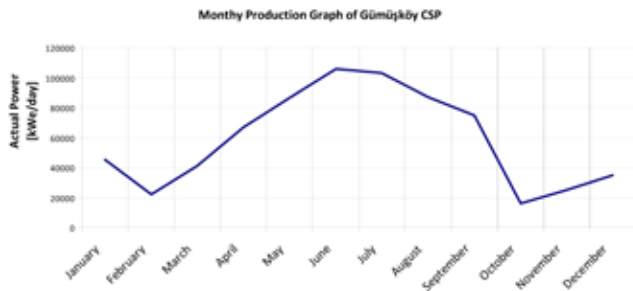


Figure 5. CSP daily net production capacity variation throughout the year

HYBRID PLANT DESIGN

The design was developed based on the working fluid superheat concept, by utilizing solar-derived heat to raise the temperature of the working fluid in the geothermal power generation cycle before it enters the turbines.

In the original GK GEPP design, the separators are located at individual well-heads. Geothermal brine is then transmitted to the power plant through separate transmission pipes in liquid and steam phases, also having two separate heat exchangers for each phase. A third heat exchanger was added to the binary loop in order to allow exchange of the solar-derived heat before transmitting the brine to the turbines. Superheated vaporized binary working fluid is then passed through the turbines, condensed through air cooled condensers and pumped back to the geothermal heat exchangers by circulation pumps (Figure 6).

Solar field capacity was selected based on the peak power deficiency (i.e. difference between design capacity and minimum production capacity) calculated from the Power Plant annual net production capacity variation (Figure 3) for the months of July and August. Next, the enthalpy amount corresponding to this production deficiency was calculated.

Lastly, the amount of required CSP solar field was calculated in consideration of numerous manufacturers' specifications and the local solar radiation levels (Table 1).

A perusal of the annual net power variation graph shows that in certain times having cool (favorable) weather conditions as well as relatively strong solar radiation levels, the hybrid system produces above the power generation capacity of the power island (Figure 7). Some of the generated heat is therefore wasted during spring and autumn.

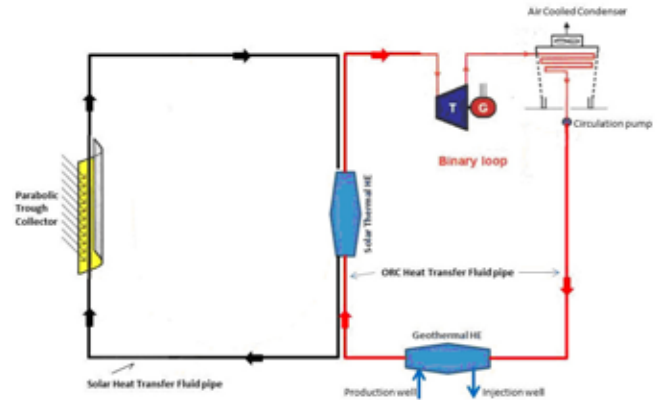


Figure 6. Gümüşköy Hybrid GEPP Proposed Cycle Diagram

Table 1. Solar Field Size Calculation Table

| Design Item | Calculated Value for Hybridization |
|--|------------------------------------|
| Average ambient temperature | 28.67°C |
| Peak power deficiency | 2,145.0 kW _e |
| Thermal power deficiency | 19,500.0 kW _t |
| Thermal power def. incl. heat exchanger losses | 22,941.2 kW _t |
| Design solar radiation | 900 Wt/m ² |
| Solar field efficiency | 63% |
| Total required solar field area | 40,000. m ² |

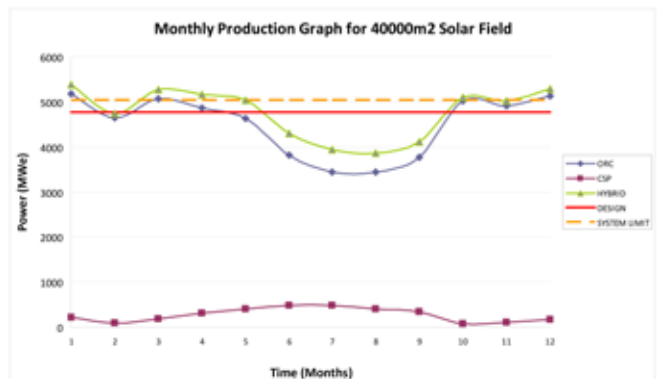


Figure 7. Annual net power variation for GEPP, CSP and HYBRID for Alternative 1 with 40,000 m² solar field area

Further trials were performed with reduced solar field levels in order to optimize the total LCOE, where solar field sizes of 50,000 m² (alternative 2) and 30,000 m² (alternative 3) were utilized (Figures 8 and 9).

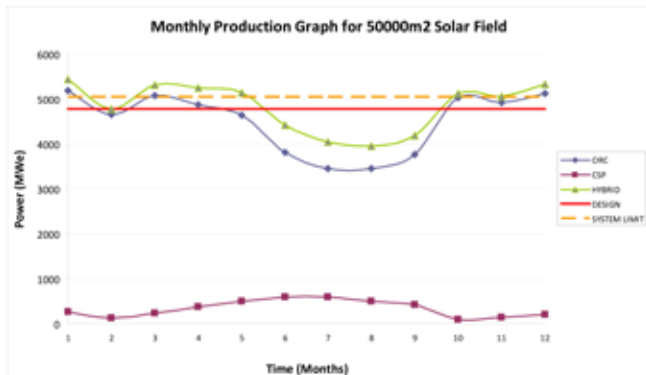


Figure 8. Annual net power variation for GEPP, CSP and HYBRID for alternative 2 with 50,000m² solar field area

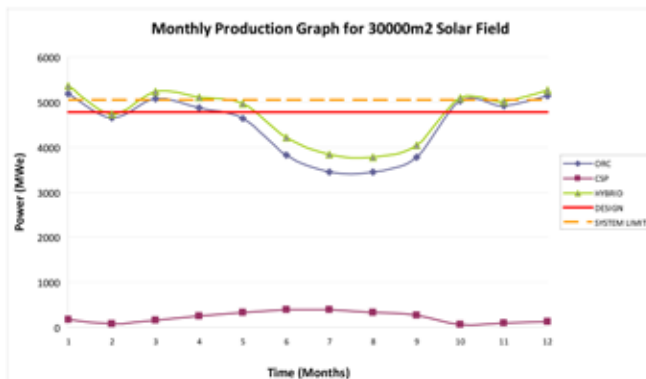


Figure 9. Annual net power variation for GEPP, CSP and HYBRID for alternative 3 with 30,000m² solar field

Operational data can be calculated as presented in Table 2 below.

Table 2. Project Performance

| | Total Annual Production (kWh)[1] | Plant Efficiency |
|-------------------------|----------------------------------|------------------|
| ORC | 54,385,340.00 | 0.949 |
| CSP (Alt.3) | 2,631,959.00 | 0.267 |
| Hybrid (Alt.1) 40000 m2 | 57,113,592.00 | 0.996 |
| Hybrid (Alt.2) 50000 m2 | 57,245,800.00 | 0.999 |
| Hybrid (Alt.3) 30000 m2 | 56,541,601.00 | 0.986 |

[1] Theoretical production above the system limit have been excluded in the annual power generation calculations.

PROJECT ECONOMICS

Project economics have been calculated by determining CAPEX and OPEX values for 3 hybrid alternatives containing 3 different solar field sizes, coupled with the 6.6MWe Gümüşköy geothermal power plant.

Calculated values by utilizing price assumptions of 10.5 cents/kWh electricity, \$127/m² for solar thermal collectors (based on an indicative tender study comprising 3 vendors), and 7% annual interest rate as commonly applied for renewable energy projects are given in Table 3. The electricity rate is based on geothermal energy feed-in tariff rates currently implemented in Turkey. Solar thermal prices are higher at 13.3cent /kWh, however these were not considered

for the solar generated part in order to stay on the conservative end of possible legislative limitations.

Table 3. Project Economics

| | Cost of Plant (USD) | Annual power generation (kWh) | EBITDA (USD) | IRR (%) |
|------------------------------------|---------------------|-------------------------------|--------------|---------|
| ORC | 20,000,000 | 42,299,286 | 4,441,424 | 17.37 |
| CSP (Alt.3) | 5,090,000 | 2,631,959 | 276,355 | - |
| Hybrid (Alt.1) 40000m ² | 25,090,000 | 44,417,240 | 4,663,810 | 13.92 |
| Hybrid (Alt.2) 50000m ² | 26,362,942 | 44,524,065 | 4,733,753 | 13.30 |
| Hybrid (Alt.3) 30000m ² | 23,817,765 | 43,909,809 | 4,610,530 | 14.72 |

DISCUSSIONS & CONCLUSIONS

The above calculations show the most favorable returns from Alternative 3 (30,000 m² solar field area) with an IRR of approximately 14.72% for hybridization of the Gümüşköy GEPP project. On the other hand as this is an early study, further work is required on the following:

- An unregulated CSP applications would take 2-3 hours for the working fluid to reach the superheating temperature (150°C or above), which would lose valuable time from the high solar radiation time zone. A better solution would be to utilize a portion the geothermal system's still high production efficiency during cool morning times and for rapidly heating the CSP working fluid to operating temperature. This can be accomplished by allowing the system to run in reverse (having the CSP heat exchanger cool the geothermal system) for a short period each morning. The net effects of this configuration have to be analyzed in the succeeding study.
- It was noted total enthalpy produced by the hybrid system exceeds the peak power generation capacity of the power island during some spring and autumn days and an optimization was performed with reduced solar field sizes. However, these calculations were carried out only as rough approximations based on daily average temperatures and not hourly temperatures. Figure 10 shows the significant waste and certain gaps formed by hourly variations, which means a more detailed optimization that will calculate total annual energy generation in consideration of all hours of the year is required for investment-grade accuracy.
- An analytical modeling tool (for estimating efficiency, energy generation and financials including benefit/cost, LCOE for different fields and resources) is seen as the next helpful step for better optimizing for system configuration, equipment selection and size selection functions. This tool would also serve as the stepping stone for adapting the hybridization scheme to other low to medium enthalpy geothermal fields.

A lot of exploration work goes to waste owing to below ideal temperatures discovered in the reservoirs. By superheating these geothermal fluids via CSP, energy generation from these resources can also be made viable. This would potentially increase any geothermal countries' energy generation potential and jump start a high number of new power projects as well as risky exploration initiatives. In both cases of energy generation, the projects' economic viabilities increase and the projects become attractive for private funding.

Meanwhile for Gümüşköy GEPP,

- A detailed model shall be constructed in accordance with the above considerations, which yielding a positive IRR value;
- A pilot CSP field shall be coupled with the existing 6.6MWe geothermal system and run for a period of 6-12 months for observing actual production values and contribution to the overall system,
- A complete system design shall be developed and 70-80% of the design solar field size shall be integrated as Stage I, in order to compensate for any over engineering errors,
- Solar field shall be increased to full calculated size and extended to include hybridization of the second 6.6MWe unit.

Future studies may include system optimization of hybrid systems including working fluid selection, heat exchanger modifications, improved materials etc. and further optimization studies by introducing partial regulation via heat storage in order to spread excess enthalpy over to continuing deficiency zones.

EDITOR'S NOTE

This paper was originally published in the Geothermal Resources Council Transactions, Volume 36, Geothermal: Reliable, Renewable, Global, GRC 2012 Annual Meeting and reprinted with permission from the Geothermal Resources Council and authors.

REFERENCES

- Greenhut A.D., 2010. *Modeling and Analysis of Hybrid Geothermal-Solar Thermal Energy Conversion Systems*, Masters Thesis, Mechanical Engineering, Massachusetts Institute of Technology, p. 173.
- Kohl T., Speck R., 2004. "Electricity Production by Geothermal Hybrid-Plants in Low Enthalpy Areas", *Proceedings*, Twenty-Ninth Workshop on Geothermal Reservoir Engineering Stanford University, Stanford, California, January 26-28, 2004 SGP-TR-175.
- Kreuter H., Kapp B., 2008. "The Concept of Hybrid Power Plants in Geothermal Applications", *Geo-Heat Center Quarterly Bulletin*, Vol. 28, No. 3, pp. 8-9.
- Astolfi M., Xodo L., Romano M. C., and E. Macchi, 2011. "Technical and Economical Analysis of a Solar-Geothermal Hybrid Plant based on an Organic Rankine Cycle," *Geothermics*, Vol. 40, pp. 58-68.
- Ediger V. S. And S. Akar. 2007, "ARIMA forecasting of primary energy demand by fuel in Turkey", *Energy Policy*, Vol. 35 pp.1701-1708.
- Kaygusuz K., 2011, "Prospect of concentrating solar power in Turkey: The sustainable future", *Renewable and Sustainable Energy Reviews*, Vol. 15, pp. 808-814
- Lentz A. and R. Almanza. 2006, "Solar-Geothermal Hybrid System," *Applied Thermal Engineering* Vol. 26, pp. 1537-1544.
- Mertoglu, O., Simsek, S., Dagistan, H., Bakir, N., and N. Dogdu. 2010. "Geothermal Country Update Report of Turkey (2005-2010)," *Proceedings of the 2010 World Geothermal Congress*, Bali, Indonesia, April 25-29, 2010, paper No. 0119, 9 pp.
- Şimsek, S., Mertoglu, O., Bakir, N., Akkus, İ., and O. Aydogdu. 2005, "Geothermal Energy Utilization, Development and Projections-Country Update Report (2000-2004) of Turkey," *Proceedings*, World Geothermal Congress 2005, Antalya, Turkey, 24-29 April 2005.
- Serpen U., Aksoy N. And T. Ongur. 2010. "Present Status of Geothermal Energy in Turkey," *Proceedings*, Thirty-Fifth Workshop on Geothermal Reservoir Engineering Stanford University, Stanford, California, February 1-3, 2010 SGP-R-188.

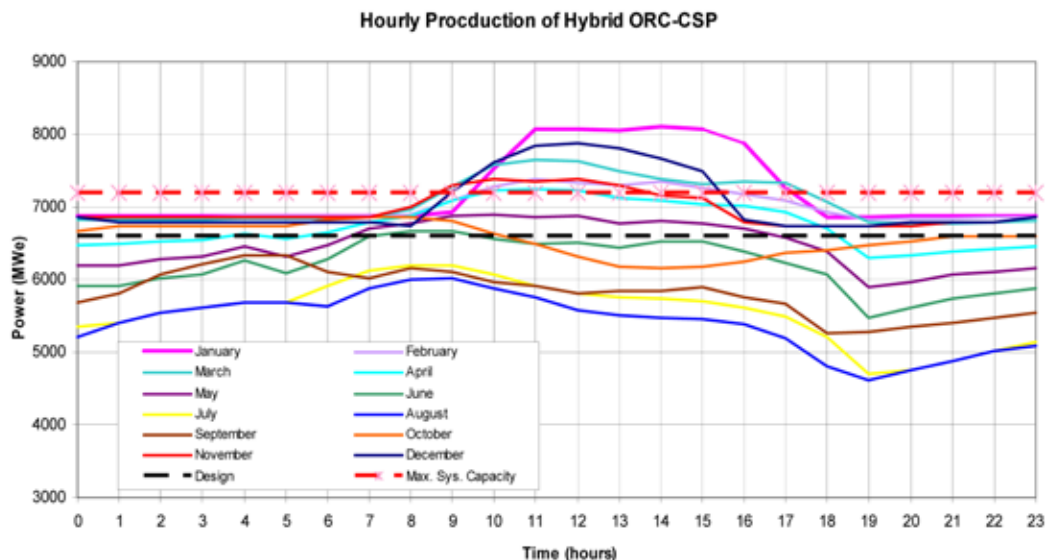


Figure 10. Hourly net power variation for the hybrid system vs. max. system capacity (upper dashed line)

A THERMOELECTRIC-BASED POINT OF USE POWER GENERATOR FOR STEAM PIPES

R. Dell, C.S. Wei & G. Sidebotham, The Cooper Union, New York, New York, USA
Magnus Thor Jonsson & Rúnar Unnþórsson, University of Iceland, Reykjavík, Iceland

ABSTRACT

A robust thermoelectric-based point of use power generation system with no moving parts that is designed to be clamped onto the outer wall of a steam pipe with a temperature of 160°C plus was built and tested in ambient temperatures from 30 to 85°C. The system consists of a pair of assemblies mounted on opposite sides of a pipe. Each assembly consists of a hot block, an array of three thermoelectric modules wired in series and a cold block heat pipe system. The steel hot block creates a thermal channel to the hot plates of the modules. The cold block consists of a 35 centimeters long heat pipe onto which 41 square fins are attached with a spacing of 0.6 centimeters. The first iteration produced a steady state direct current voltage of 17.2 (open circuit) and an amperage of 0.64 (short circuit) after more than a year of continuous operation. Later versions produced 31.5 volts (open circuit) and 0.89 amps (short circuit), and 21.36 volts open circuit volts and 1.14 short circuit amps in steady state. Additional installations using low temperature geothermal steam and hot water pipes in Iceland were also successful with ambient temperatures below zero degrees Celsius. For comparison purposes with other thermoelectric generators, this thermoelectric generator system produces more than 1 watt per thermoelectric module without any moving parts. These thermoelectric generators produce 6.9 watts steady state and the higher amperage unit produces 6.1 watts steady state.

INTRODUCTION

Geothermal power plants often employ monitoring systems at remote locations that require DC power. If available, standard AC power is easily converted to the required DC power. If not, a separate power line must be installed and maintained. DC power sufficient to run modern telemetry can be obtained by placing the hot block of a thermoelectric power system onto the exterior of a typical exposed steam pipe. A thermal image of a vortex steam meter is shown in Figure 1. The exterior temperature of the exposed pipe is of the order of 160°C. The ambient temperature of an enclosed space with steam pipes can approach 60°C, giving an available temperature difference between the high temperature source and low temperature sink on the order of 100°C. Greater temperature differences increases the system's power production.

A thermoelectric power system (Figure 2) consists of a thermoelectric module, a circuit load (r_L), a high temperature heat transfer channel (hot block) and a low temperature heat transfer channel (cold block). The two heat transfer channels are required to maintain the temperature difference between the two plates.

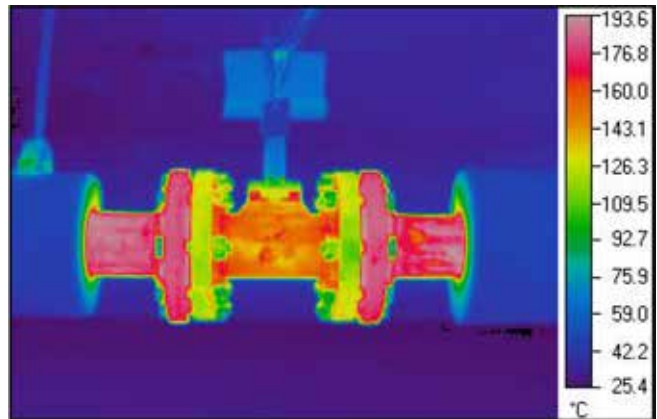


Figure 1: Thermal Image of Exposed Steam Pipe and Steam Meter.

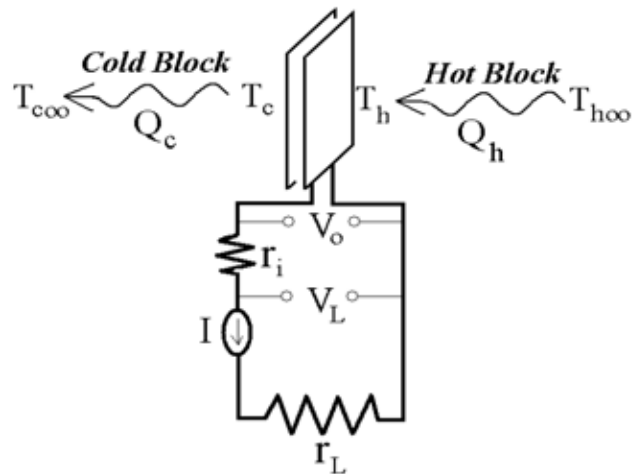


Figure 2: Schematic of a Thermoelectric Power System. The module is modeled electrically as a voltage source (V_o) with an internal resistance (r_i)

MATERIALS AND METHODS

The thermoelectric power system is protected by European Patent Application No. 07862348.5, United States Patent Application 20080142067 and Canadian application 2671995. Preliminary per unit costs estimates are under \$1,500 per unit.

Each assembly consists of a hot block, a module array, and a cold block. Figure 3 shows an exploded view of the generator assembly (left), assembled generator (center), and the generator mounted on a steam pipe (right).

The entire unit mass is 4.7 kilograms. The cold blocks' (heat pipes) mass is 3 kilograms. The remainder is the hot blocks and the thermoelectric modules. The dimensions are 52 centimeters along the pipe, 45 centimeters wide and 22 centimeters high. Unit variations permit mounting on vertical and oblique angle pipes.

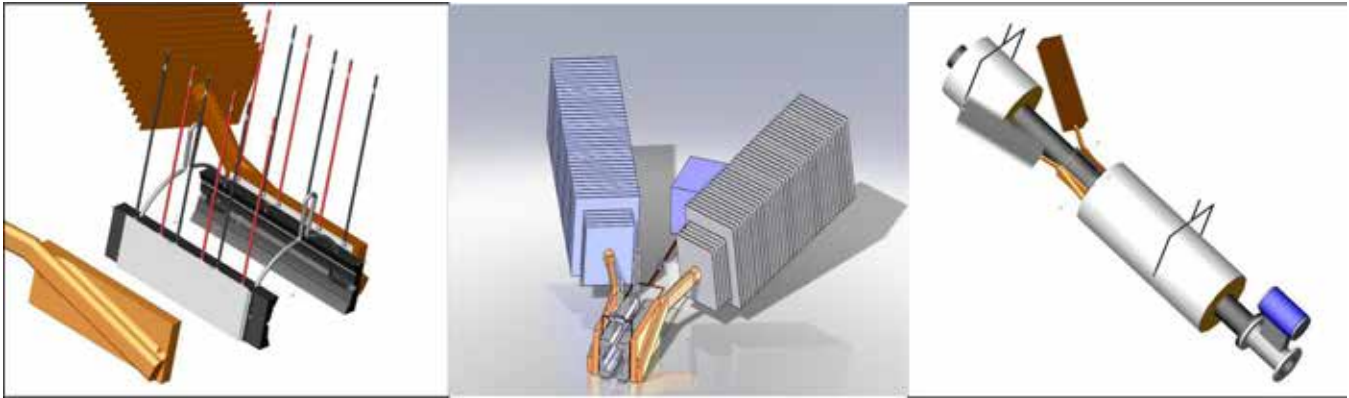


Figure 3: Solidworks rendering of the Thermoelectric Power System. It shows an exploded view of the generator assembly (left), assembled generator (center), and the generator mounted on a steam pipe (right).

Steam Pipe Connection

As shown in Figure 4, a clamp-on system was developed that could be readily attached directly to the surface of existing steam pipes. This low cost solution does not violate the existing steam system's integrity and as such precludes many safety and inspection considerations. The steam pipes surface is hand sanded with 120 grit sandpaper and then cleaned with damp cloth, followed by a solvent wipe. Both the hot blocks and the pipe are covered with Arctic Silver Ambrosia thermal grease. This simple installation protocol together with the clamping and onsite wiring take less than one man hour to complete.

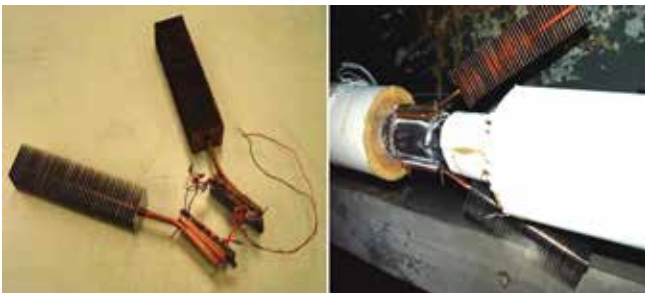


Figure 4: Photos of Thermoelectric Power System. Left photo is assembled, not mounted. Right photo is mounted on a bare section of steam pipe, as seen from underneath the generator.

Thermoelectric Modules

Laird Technologies Incorporated, a major developer of thermoelectric modules (TEMS) several years ago achieved a technical breakthrough in the development of high temperature modules that are designed to function in the temperature ranges of steam systems. These new modules meet U.S. Military specifications.

Although originally designed for thermoelectric cooling, TEMs can be used in reverse. In a cooling mode, electricity is added, and heat is transferred (or pumped) from one flat surface to the other. We use these in reverse, by creating a temperature difference between the two flat surfaces. Extra care must be taken in the engineering design and the assembly protocol to create a maximum temperature difference between the two flat surfaces of the TEMs. Ideally, a vacuum on the edges of the modules would be maintained. This

project uses special tolerance lapped modules that can be assembled in units of three TEMs. The assembled generator uses six TEMs. The current configuration has the TEMs wired in series.

The end result is a generator that is so effective that changes of airflow are immediately manifest by voltage fluctuations. For each 10°C of temperature change in the ambient temperature causes approximately 1 volt change in generated power. To maintain a more constant voltage and to create a power reservoir, a voltage regulator with trickle charge capability can recharge a battery.

Hot Block

The main function of the hot block (Figure 5) is to provide a curved surface to mount onto the exterior of a steam pipe, and a flat surface on which to mount thermoelectric modules without adding significant thermal resistance.

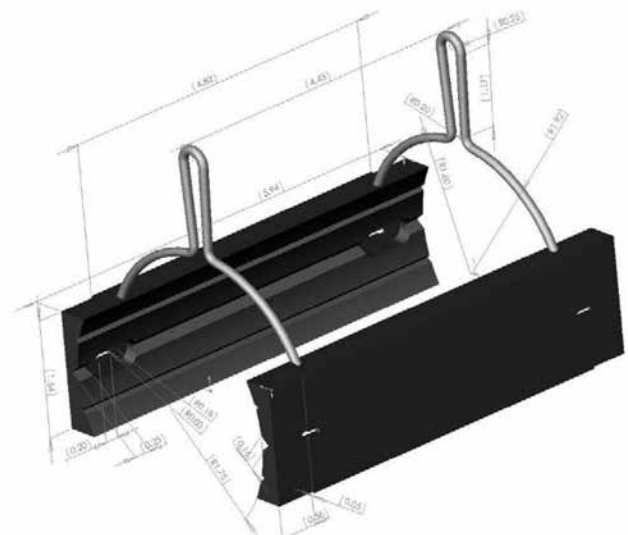


Figure 5: Solidworks rendering of a pair of hot blocks connected by 2 cradles.

Steel was chosen as the material for the hot block because the steam pipe is also steel. This choice eliminates any difference in the expansion and contraction rates, thus insuring no additional movement of the thermal interfaces

that are coated with thermal grease. This solution also eliminates any potential galvanic reactions between the steam pipe and the hot block, and the thermal grease serves as an additional galvanic barrier. Prototype brass hot blocks for brass pipes have been fabricated and tested.

Parallel grooves were cut into the curved surface of the hot block. This helps to mitigate any difference in radius. It also minimizes any hot block warpage that could degrade the interface with the TEMs. These grooves serve a third function in providing a channel for the expulsion of any excess thermal grease.

The milled surface of the hot block was recessed to form a channel for the TEMs, which are oscillated into position with thermal grease between the surfaces. This enables precise control of the TEMs position while enhancing the unit's efficiency due to enhanced air circulation.

Two hot blocks are joined together, separated by an inverted stainless steel cradle system that is shaped to facilitate proper alignment on the steam pipe. This eliminates any possibility of steam pipe warpage due to an uneven pipe surface temperature. The cradle also serves as a spring that holds the unit in place during the clamping process. The top spring section serves the additional function of providing gripping points for the installation process, thus minimizing any unnecessary contact with the hot steam pipe.

All wiring of the TEMs can be completed before the installation, with the cradle serving as a mounting point for the wire harnesses.

Thermal Grease

Traditional thermal greases quickly dry at steam temperatures and are not recommended for these applications by the manufacturers. Arctic Silver has developed a high-temperature thermal grease, Ambrosia HT that was modified to our specifications for this project. This product is unique in that it contains nano particles that settle into any voids over a period of approximately 100 hours, thereby potentially creating an increase in system power generation after the unit is initially installed.

Cold Block

The main function of the cold block system is to provide a thermal channel between the cold plate of the thermoelectric module array and the ambient environment. Since the mode of heat transfer ultimately involves the convective/radiative transfer of heat from a solid to ambient air, the thermal goal is to provide a large exposed surface area of material as close to the cold plate temperature as possible.

The cold block system was fabricated by Noren Industries. The system's design consists of a copper mounting block (with one surface mounted on the thermoelectric module array), and a heat pipe onto which evenly spaced rectangular fins are mounted. There is a physical restriction in that the internal flow relies in part on gravity, and it performs poorly if placed horizontally. A mild angle (i.e. 15 degrees from

horizontal) is sufficient for the heat pipe chosen. Rectangular fins are mounted onto the heat pipe. The system chosen relies primarily on natural convection, and a restriction on the fins is that they be nearly vertical to allow the flow to accelerate vertically between them. Also, the spacing must be sufficiently large that there is minimal interference between the thermal boundary layers of adjacent fins.

The system consists of two mirrored heat pipes that are splayed back along the steam pipe (Figure 6). This decreases the amount of heat pipe that protrudes into the workspace around the steam pipe. This geometry is important for safety concerns and it enables installation in a one square foot envelope around the steam pipe.

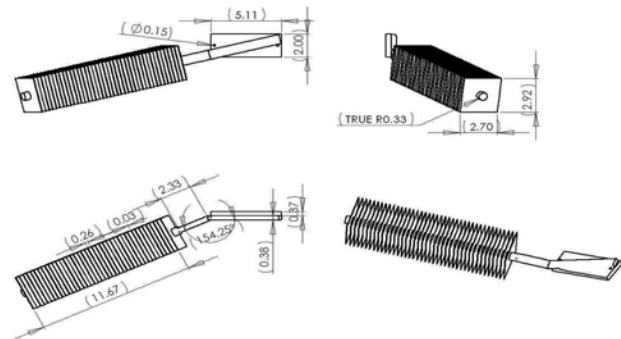


Figure 6: The cold block system.

RESULTS AND DISCUSSION

The first test bed (The Cooper Union's steam room at The Albert Nerken School of Engineering, 51 Astor Place) had a summer temperature of approximately 52°C at an elevation of 1 meter above the floor in the summer and 46°C in the winter. The 3 inch steam pipe had a surface temperature of 158°C. Temperatures were measured using a Linear Labs C-1600 non contact infrared thermometer, a Fluke 867B graphical multimeter with a temperature probe, and a Mikron 7200 thermal camera. Electrical measurements were taken with a Fluke 867B graphical multimeter, and a Fluke 87 multimeter.

The system output voltage and current were measured when the system was used to drive two different light bulbs. Figure 7 shows the experimental operating line of the system on a Voltage vs. Current plot. The point on the voltage axis (zero current) is the open circuit voltage of 17.2 V, and the point on the current axis (zero voltage) is the closed circuit current (0.63 Amps). The plot is linear between these two points, with a slope equal to 24.4 Ohms.

Figure 8 shows open circuit voltage (over a two hour period) and closed circuit current (over 10 minutes) obtained from the system as a function of time. The output is stable. An improved version of the generator produced 12.4 volts open circuit volts and 0.81 short circuit amps in steady state using only one half (one side) of the generator - 3 thermoelectric modules. The voltage would be doubled in a full unit (12 volts per side) because the modules are connected in series. Figure 9 shows the Iceland installation.

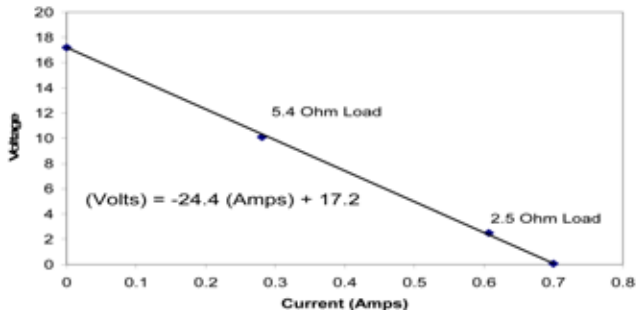


Figure 7: System voltage as a function of Current for various electrical loads.

To provide a backup, higher peak power and stable voltage, a battery cell that is charged by the generator under load a trickle charge system using a Xantrex 3-phase (bulk, absorption and float) unit was tested, as shown in Figure 10. A 12-volt 7 Ah (amp-hour) sealed lead acid rechargeable battery and a Manson SBC – 7112 PV charge controller was used.

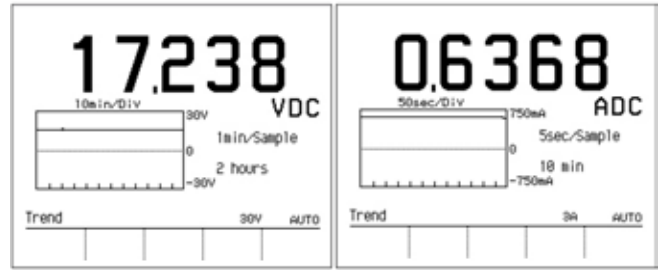


Figure 8: System voltage (open circuit) and current (short circuit) as a function of time.

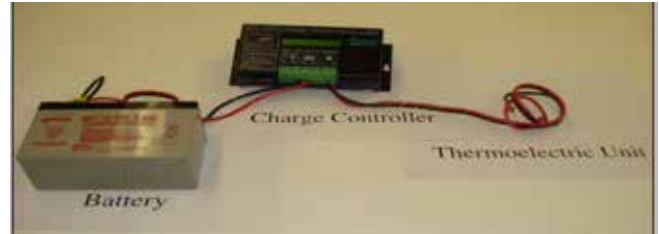


Figure 10: The backup battery cell.

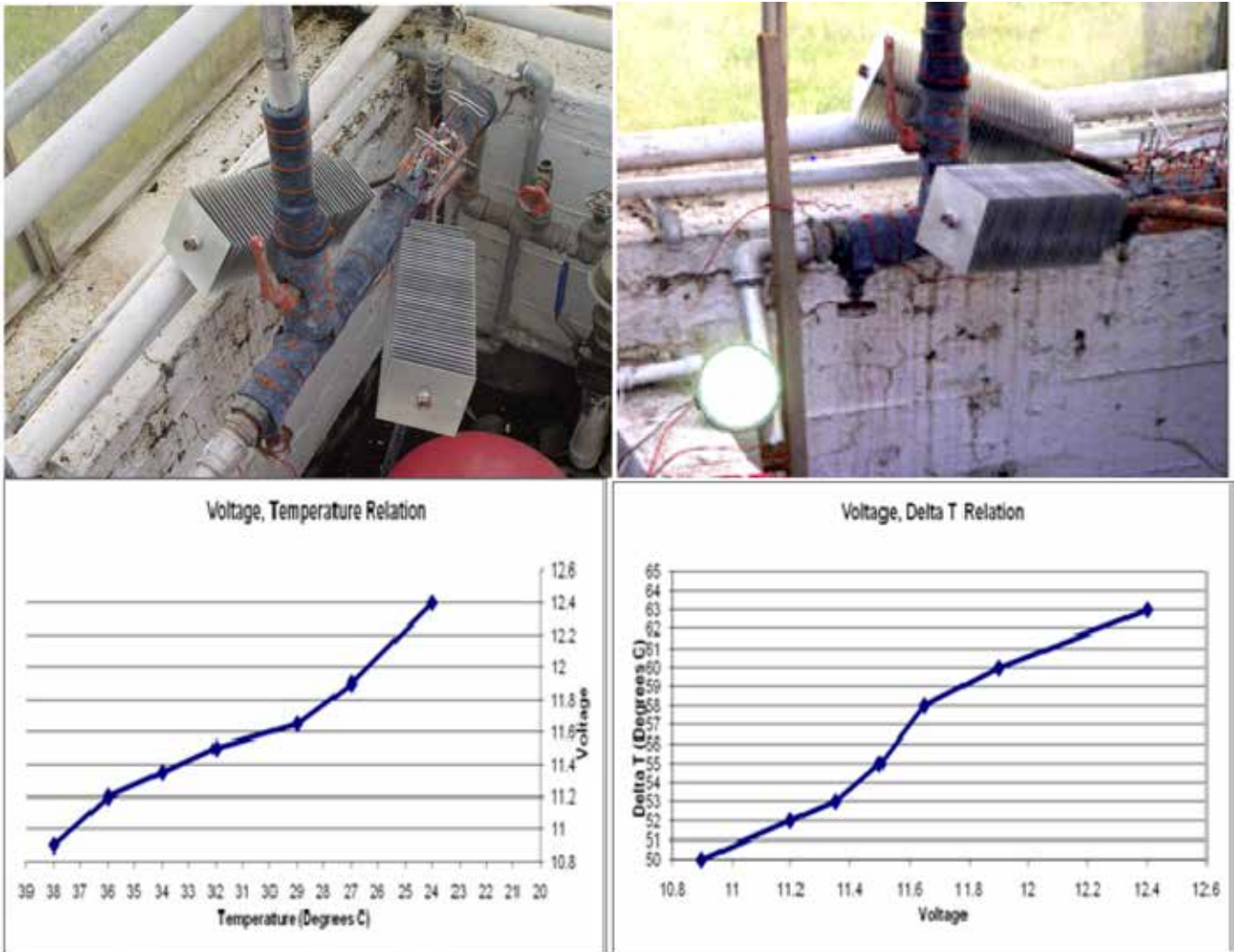


Figure 9: Iceland installation using geothermal steam and condensate mix at 100°C (top left), powering an LED light fixture (top right); temperature vs. voltage (bottom left); delta T vs. voltage (bottom right)

An improved unit was installed in another steam room with an ambient temperature of approximately 30°C at an elevation of 1.2 meters above the floor. The steam temperature was 160°C. It produced 31volts open circuit volts and 0.89 short circuit amps in steady state. The most recent configuration uses high amperage thermoelectric modules. At our new test bed, it produces 21.36 volts open circuit volts and 1.14 short circuit amps in steady state with similar temperature parameters (Figure 11).



Figure 11: Shows the system voltage (open circuit) and current (short circuit) for the improved unit.

The total watts produced by a thermoelectric generator can be approximated by multiplying the open circuit voltage by the short circuit amperage and then divide the product by 4. The improved unit produced 6.9 watts steady state and the higher amperage unit produces 6.1 watts steady state. For comparison purposes with other generators, our thermoelectric generator produces slightly more 1 watt per thermoelectric module.

As a demonstration of the generator's utility, a Y-cam Solutions Ltd. S-range Indoor IP security camera YK004 was connected to the system. The camera was successfully powered and transmitted surveillance images to an internet-enabled laptop computer.

CONCLUSIONS

A robust thermoelectric-based point of use power generation system with no moving parts that produces more than 6 watts of steady state power is now available. There are many potential locations for this system in the geothermal industry, including existing steam pipes and remote installations on municipal district heating pipes. The performance, low cost, and ease of installation of this generator enables the installation of reduced power telemetry and security camera systems.

ACKNOWLEDGEMENTS

This work was conducted under the auspices of the C. V. Starr Research Foundation and the Center for Innovation and Applied Technology at the Cooper Union for the Advancement of Science and Art. Facilities were provided by the Cooper Union, the Keilir Institute of Technology, and the Agricultural University of Iceland. The funding and support of Consolidated Edison, Laird Technologies Inc, Arctic Silver and Noren Heat Pipe is greatly appreciated.

The contributions of the following Student Research Assistants are greatly appreciated: William Foley, Alex Bronfman, Anthony Morris, Subashis Paul, Kelly Smolar, Brian Theodor, Luis Vasquez, Beatrix Ponce, Gina Magnotti, Takuya Otani, Samantha Massengill, William Witter, Raymond Bekheet, Beatrix Ponce and Craig Stevenson.

REFERENCES

Fundamentals of Engineering Thermodynamics. Sixth edition, Moran, Michael J. and Shapiro, Howard N., Wiley & Sons, Inc., Hoboken, N J, 2008.

Thermocouples: Theory and Properties, Pollock, Daniel D. CRC Press, New York, NY, 1991.

A Geothermally Driven Peltier Generator for Powering Instruments and Transmission Link from Vantajokull Glacier, Jon Sveinsson, Magnus T. Gudmundsson and Finnur Palsson (Veggspjald), Conference on Industrial Uses of Geothermal Energy Reykjavik. Iceland 1992

Heat Pipes, 4th edition, Dunn, P. D. and Reay, D. A., Pergamon Press, Tarrytown, NY, 1994

"Small Thermoelectric Generators." *The Interface*, Electrochemical Society, Pennington, NJ, 2008

CRC Handbook of Thermoelectrics, D.M. Rowe, CRC Press, New York, NY 1995

"Thermoelectric Power Generation Using Waste-Heat Energy as an Alternative Green Technology", Basel I. Ismail, Department of Mechanical Engineering, Lakehead University, & Wael H. Ahmed, Canada, Component Life Technology, Atomic Energy of Canada Ltd., Canada, 2008

<http://www.benthamsience.com/eeng/samples/eeng2-1/0004EENG.pdf>

USES AND ADVANTAGES OF GEOTHERMAL RESOURCES IN MINING

Piyush Bakane, Department of Mining and Metallurgical Engineering, University Of Nevada, Reno, Nevada

ABSTRACT

Economic production of minerals along with production of electric power from geothermal power plants can be termed as cascade use of geothermal power plants. Minerals like silica, lithium, manganese, zinc and sulfur can be removed from geothermal fluid or steam to obtain marketable byproduct; these minerals are also a major source of corrosion and scaling which leads to mechanical failures. Methods of metal extraction developed previously and its importance for power plant to operate efficiently will be discussed here.

INTRODUCTION

Geothermal energy is defined as energy stored inside the earth crust. This energy is in the form of high temperature. Because of the magma, rock near to it gets heated and we get molten rocks with minerals in it. This molten rock interacts with rain water which percolates through major faults and fractures results in the formation of a dilute brine (Figure 1).

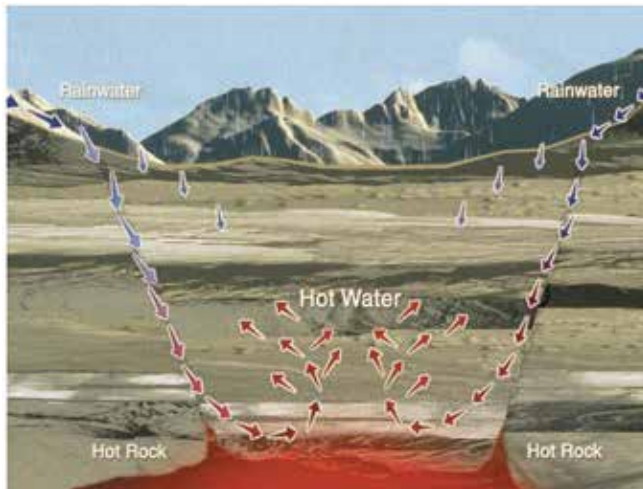


Figure 1. Percolation of rain water into fracture and its reheating due to hot rocks (GEO, 2000).

These resources can be increased if we can extract more energy from low temperature reservoir. New technologies are introduced which will help to extract more and more energy from earth. New technologies such as Enhanced Geothermal Systems (EGS) are helping us to extract more heat from areas where there is less availability of underground water.

Geothermal fluid with a range of 200°F (93°C)(low temperature) to 400°F (204°C)(high temperature) can be used for hydrothermal electricity (Kagel, 2008).

Due to the fault formation and other geologic reasons, subsurface temperature of Nevada and California is very high. Besides these regions are rich in minerals which are water soluble. When such minerals are subjected to high pressure and temperature mineral becomes soluble and we get a fluid which has all these water soluble minerals.

GEOTHERMAL AND MINING INDUSTRY

Geothermal fluids interact with the host rocks and tend to become increasingly saturated with various minerals. Some geofluids are rich in minerals and some are free of minerals. Geothermal fluids are mostly water, steam or combination of two. Geofluids are generally hot, salty (because of the mineral content). Any of these fluids acts as a carrier to get geothermal energy up through wells from subsurface to surface.

The resulting chemical compositions of geofluids are determined by:

- Composition of rocks
- Chemical composition of fluid.
- Temperature and pressure during the fluid and rock mass interaction.

NaCl, NaSO₄ and Na/CaCO₃ are some of the major geothermal fluids which are present in Nevada (Trexler, et al., 1990)

Due to large availability of geothermal resources in Nevada and California, geofluid can be used for the extraction of water soluble minerals as well as precious metals.

For example:

1. The use of geothermal fluid in heap leaching for silver and gold extraction. (Trexler, et al., 1990).
2. Extraction of silica from geothermal power plant. (Parker, 2005).
3. Mining lithium from geothermal 'lemonade'.
4. Collection of sulfur from geothermal steam (Li and Brouns, 1978).

Table 1 shows some examples of mineral composition of selected geothermal fields. Figure 2 shows the temperature distribution throughout the USA for use of geothermal.

Table 1. Examples of mineral composition of selected geothermal fields (Bouncier, et al., 2003 and Gallup, 1998).

| | Salton Sea, CA | Coso, CA | Dixie Valley, NV | Mammoth Lake, CA |
|-----------------|----------------|----------|------------------|------------------|
| Temp. (°C) | 296 | 274 | 246 | 165 |
| Silica (mg/kg) | >461 | >711 | >599 | ca 250 |
| Boron (mg/kg) | 257 | 119 | 9.9 | NA |
| Lithium (mg/kg) | 194-230 | 45 | 2-4 | NA |
| Zinc, (mg/kg) | 438 | 0.03 | NA | NA |

Also geothermal energy is used in a number of industrial applications such as pulp, paper and wood processing, diatomite plant, vegetable hydration and waste-water treatment.

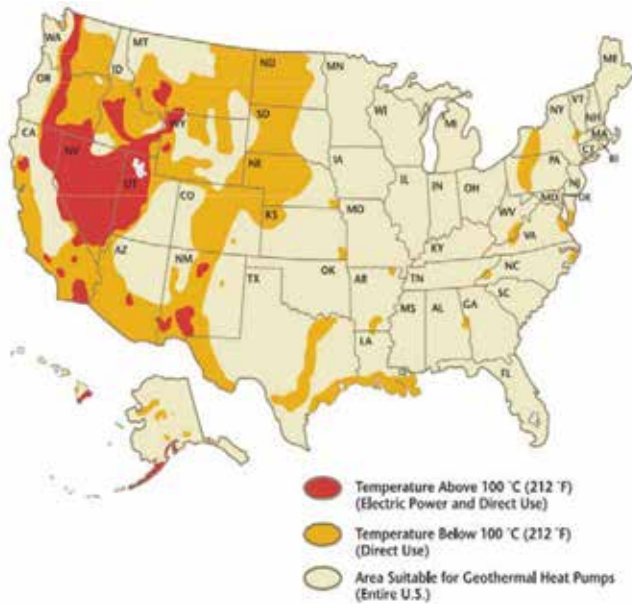


Figure 2. Temperature distribution throughout the USA for use of geothermal (Green and Nix, 2006).

EXTRACTION OF GOLD, SILVER USING HEAP LEACHING WITH THE HELP OF GEOTHERMAL FLUID

Heap leach is an industrial process which is used to extract precious metals such as gold, silver, etc. Heap leaching of gold and silver ores is conducted at approximately 120 mines worldwide (Kappes, 2002). The main advantage of heap leaching is low capital cost. Around 12% of the gold is produced with the help of heap leaching process. Nevada is known as the birthplace of the heap leaching process. Modern day leaching was started in Nevada in 1960 (Kappes, 2002). Figure 3 shows the schematic diagram of the thermally enhanced heap leach process.

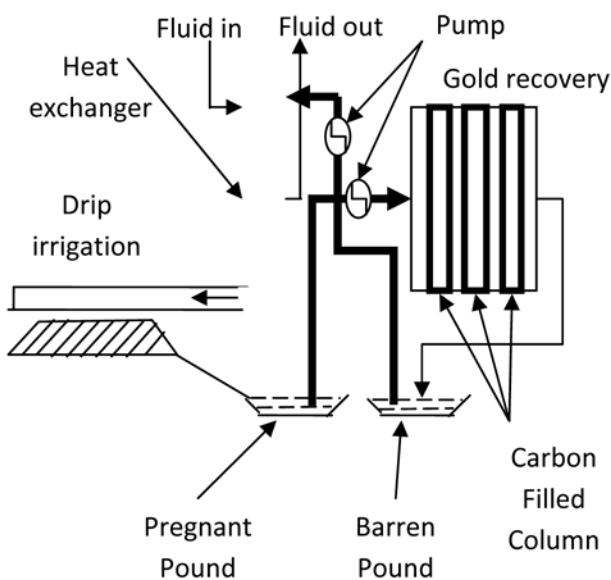


Figure 3. Idealized thermally enhanced heap leach (Trexler, et al., 1990)

Heap leaching may be defined as stacking of metal-bearing ore into a “heap” on an impermeable pad, irrigating the ore for an extended period of time with a chemical solution to dissolve the sought-after metals, and collecting the leachant (“pregnant solution”) as it percolates out from the base of the heap (Kappes, 2002).

Pregnant solution is pumped through activated charcoal at the process plant, which absorbs gold and silver. Cyanide solution is pumped to a holding basin, where lime and cyanide are added to repeat the leaching process. Gold bearing charcoal is chemically treated to release the gold and is reactivated by heating for future use. The resultant gold bearing strip solution, more concentrated than the original pregnant cyanide solution, is treated at the process plant to produce bar of impure gold. The gold is sold or shipped to a smelter for refining. The heap leaching process uses hot geofluid which is available in most of the parts of Nevada. For example, gold ore from the Freeport Jerritt Canyon Mine in northern Elko county and silver ore from Gooseberry Mine in Washoe County used to use the thermally-enhanced cyanide heap-leaching operation (Flynn, et al., 1986)

Geothermal fluid can be used for direct heating or indirect heating. During indirect heating, pipes carrying hot fluid can be laid throughout the heap leach pad to keep the heap leach pad warm and enhance the chemical processes by providing a higher temperature. While, in case of direct heating, geothermal fluid is directly circulated through leach to get the same results as that of indirect heating. During direct use of the geofluid some chemistry related difficulties may arise because of the chemical composition of geofluid. Geofluid may contain some metals and non-metals which has the ability to react with cyanide which is a major chemical component in heap leaching process. Non precious metal and non-metal which may react with cyanide to create precipitate and disturb the chemical process by plugging the cyanide dripping through the leach pad are called cynocide (Bloomquist, 2006). Amount of cynocide is also important, if the amount is not much, cynocide will not stall leaching process.

ADVANTAGE OF USE OF GEOFLUID IN HEAP LEACHING

Due to the heating of the chemicals recovery of the precious metal is speeded up. Also because of the temperature enhancement the mine operator can operate the leaching pad throughout the year. The above two reasons will help the mine operator to generate more revenues and will give year round employment opportunities. Heating of the cyanide solution will help to enhance gold and silver recovery by 5 to 7% (Bloomquist, 2006).

EXTRACTION OF SILICA FROM GEOTHERMAL POWER PLANT

Extraction of silica from geothermal fluid is termed as a cascaded use of geothermal energy. Geothermal fluid contains silica which clogs tanks and pipes. So by removing the silica from geothermal fluid geothermal industry will

provide silica as a marketable by-product. And the geothermal energy will be generated. This experiment was carried out in Livermore's mobile laboratory at the Mammoth Pacific LP geothermal power plant in Mammoth Lakes, California. The Livermore extraction process involves running a geothermal fluid through a reverse-osmosis separation process to create freshwater and concentrated brine. The freshwater is used for evaporative cooling, and the concentrated brine is pumped into a reactor where chemicals are added and silica is extracted. The silica-free brine can then be pumped through another process for extraction of other metals before the fluid is pumped to a surface pond and re-injected into the subsurface (Parker, 2005).

Metals like Lithium, Manganese and Zinc can be extracted from geothermal fluid. Figure 4 shows a schematic diagram of the system which extracts silica from geofluid.

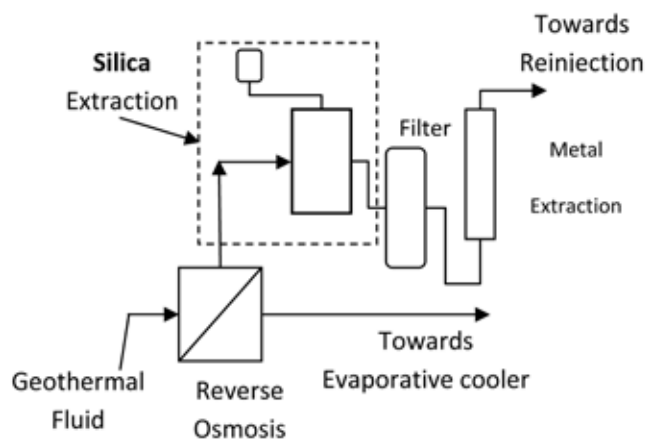


Figure 4 Extraction of silica from geothermal fluid $H_4SiO_4 \rightarrow 2H_2O + SiO_2$ (Dissolved Silica)(Quartz siliceous sinter) (Parker, 2005)

Silica production from a 50 MWe Salton Sea, California and Coso power plant, California power plant could provide \$10.2 and \$12.9 million per year respectively. These values were calculated assuming 60% silica recovery rate, a selling price of \$2200 per metric ton and a plant capacity of 95% (Bloomquist, 2006).

Removal of silica from geothermal fluid enhances the performance and reduces the maintenance cost associated with scaling in surface facilities and injection wells (Figure 5) It also facilitates the co-production of marketable minerals.



Figure 5. Scaling in geothermal pipeline (Bloomquist, 2006).

MAJOR ENGINEERING CHALLENGES BECAUSE OF THE SCALING

Temperature, pressure, chemistry and content of non condensable gases in geofluid influence the power plant operation and may affect the mechanical, volumetric and thermal efficiencies of the power plant. This will affect power production and cost per kWh. Any kind of extraneous material that appears on the inner surface of the pipe which carries a fluid is called fouling. Fouling reduces heat transfer and flow through a pipe. This affects mechanical, volumetric and thermal efficiency of the geothermal power plant. This extraneous material may react with pipe to cause corrosion. To avoid fouling the following methods can be used:

- Use of fins on inner surface of the pipe
- Use of copper-nickel alloys. Carbon steel can be used at low cost to reduce corrosion (Kagel, 2008).
- And flow rate should be managed in such way that, material should accumulate on the inner surface.

Figure 6 shows the scaled and corrode tubes from Hoch Geothermal Facility.

Reduction in fouling will help to reduce corrosion and more mineral can be extracted out on the surface.



Figure 6. Corrosion of tubes (Kagel, 2008).

EXTRACTION OF LITHIUM FROM GEOTHERMAL POWER PLANT

Because of the boost in silica extraction from geofluid, the extraction of Lithium will also turn out to be advantageous. Figure 7 shows the lithium extraction schematic diagram. In this process, fluid is extracted from production well and steam and brine are separated. The steam is then used for electricity generation. The steam condensed to cooled water. Which is reused to mix with waste brine; later this steam is sent to the Lithium Extraction Plant. After lithium extraction water is re-injected into an injection well. In this process, zinc and manganese can also be recovered along with lithium

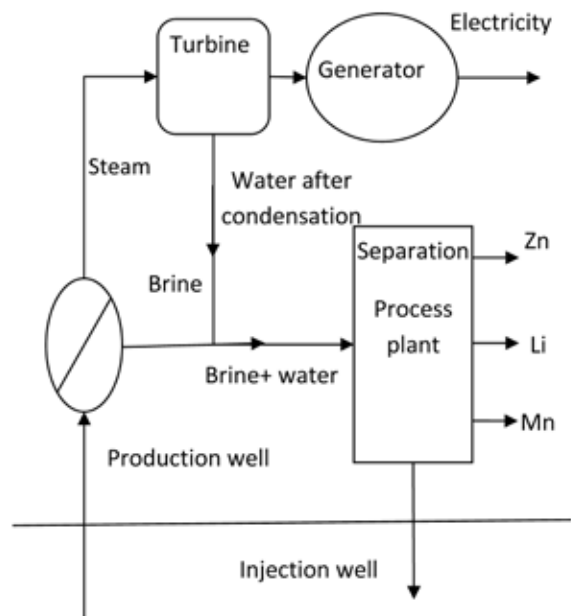


Figure 7. Lithium extraction with Geothermal Fluid (Harrison, 2010).

COLLECTION OF SULFUR FROM GEOTHERMAL STEAM

Geothermal steam contains contaminants such as CO_2 , H_2 , H_2S , NH_3 , CH_4 and N_2 . Most of these gases are not only environmentally objectionable but also they accelerate corrosion of power generating parts, which gives rise to issues like safety and increase in maintenance cost. Figure 8 shows the corroded steam vent at The old Covefort power plant.



Figure 8. Corroded Steam Vent (Kagel, 2008).

Steam containing hydrogen sulfide is purified and sulfur recovered by passing the steam through a reactor packed with activated carbon in the presence of a stoichiometric amount of oxygen oxidizes the hydrogen sulfide to element sulfur is adsorbed on the bed. The carbon can be recycled after the sulfur has been recovered by vacuum distillation, inert gas entrainment or solvent extraction. This process of purifying geothermal steam is very suitable if steam contains some other non-condensable gases. In general geothermal steam contains 99% of steam and 200 parts per million of H_2S .

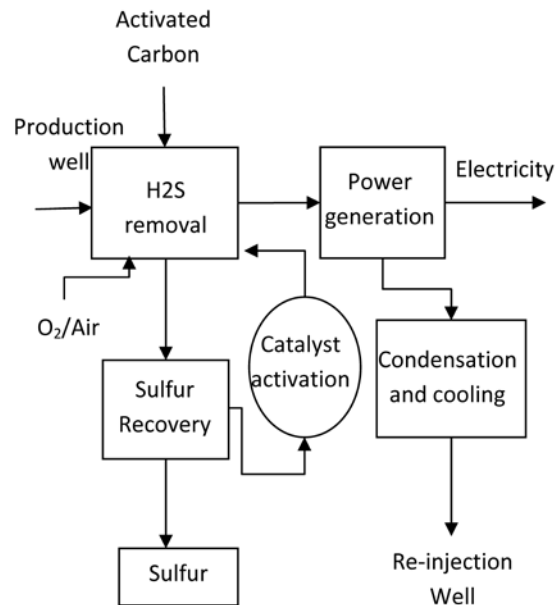


Figure 9. General Flow Diagram of the Catalytic Oxidation Process for H_2S Removal from Geothermal Steam (Li and Brouns, 1978)

ECONOMICS OF MINERAL EXTRACTION

At Mammoth Lake, preliminary data suggested that silica removal could lower the electricity generation costs by as much as one cent per kilowatt hour (Bourcier, et al., 2005). Feasibility of mineral extraction from geothermal fluid depends on the demand of that mineral in market. For example, if the supply of mineral gets more than its demand the market price of the mineral gets affected. To keep continuing the extraction of mineral it should be economical as well as profitable for the company which extracts that mineral.

CONCLUSION

Geothermal energy extraction provides various economic benefits other than its direct use such as mineral extraction. For example, approximately $35,000 \text{ m}^3$ of brine passes through a geothermal power plant facility which is around 50 MWe in capacity. Even if we consider concentration of only 1 mg/kg approximately 30 kg of metal passes through the facility each day (Gallup, 1998)

In the Salton Sea hypersaline geothermal reservoir, located in the Imperial Valley of southern California, each 50 MW geothermal power plant can also produce 16,000 tonnes of lithium carbonate equivalent, 24,000 tonnes of electrolytic manganese dioxide and 8,000 tonnes of zinc metal. According to Simbol Mining Corp, from an initial resource agreement there can be more than four 50 MW plants developed near Salton Sea (Harrison, 2010).

Geothermal is a clean source of energy. It helps power industries to generate electricity as well as reduce carbon emissions. The ability to remove silica from geothermal fluid can add to energy extraction, reduce operation and maintenance cost. Recovery of silicon opens the way for the recovery of metals like zinc, lithium, manganese, cesium, rubidium and even precious metals like gold, silver.



GEO-HEAT CENTER
Oregon Institute of Technology
Klamath Falls, OR 97601-8801

Non-Profit
Organization
U.S. Postage
PAID
Klamath Falls, OR
Permit No. 45

REFERENCES

- Bloomquist G.R., 2006, "Economic Benefits of Mineral Extraction from Geothermal Brines" *Proceedings*, International Mineral Extraction Conference.
- Bourcier, W., M. Lin and G. Nix, 2005, "Recovery of Minerals and Metals from Geothermal Fluids", Lawrence Livermore National Laboratory, Livermore, CA, USA.
- Flynn T., Trexler D. and Hendrix J., 1986, "Geothermal Enhancement of Mineral Processing in Nevada: Final Report, April 25, 1985 – June 30, 1986," University of Nevada, Reno, Division of Earth Sciences, Reno, NV, 53 p.
- Gallup, D., 1998, "Geochemistry of Geothermal Fluids and Well Scales and Potential for Mineral Recovery" *Ore Geology Reviews*, vol. 12, pp 225-236.
- Geothermal Education Office, 2000, "Introduction to Geothermal Energy - Geothermal Reservoir" <http://geothermal.marin.org/GEOpresentation/sld012.htm>.
- Green, B.D. and R.G. Nix, 2006, "Geothermal – The Energy under our Feet, Geothermal Resource Estimates for the United States", National Renewable Energy Laboratory, CO, <http://www1.eere.energy.gov/geothermal/pdfs/40665.pdf>.
- Harrison S., 2010. "Technologies for Extracting Valuable Metals and Compounds from Geothermal Fluids", *Proceedings*, Geothermal Technologies Program 2010 Peer Review, May 18, 2010.
- Kagel A., 2008, "The State of Geothermal Technology Part II: Surface Technology" Geothermal Energy Association, Washington, DC, 89 p.
- Kappes D., 2002, "Precious Metal Heap Leach Design and Practice" *Proceedings of the Mineral Processing Plant Design, Practice, and Control*, Volume 1, Society for Mining, Metallurgy and Exploration, Englewood, CO, 1606–1630.
- Li C.T. and Brouns R.A., 1978, "Removal of H₂S from Geothermal Steam by Catalytic Oxidation Process Bench Scale Testing Results" Pacific Northwest Laboratory Richland, WA 119 p.
- Parker A., 2005, "Mining Geothermal Resources-Silica Extraction" *Science and Technology Review*, Lawrence Livermore National Laboratory, CA, pp 25-27.
- Trexler D., Flynn T. and Hendrix J., 1990, "Heap Leaching" *Geo-Heat Center Quarterly Bulletin*, Vol. 12, No. 4, Klamath Falls, OR, pp 1-4.